Overview of Heavy Flavour production in DIS

Robert Thorne

November 4th 2020

University College London

I will discuss what opportunities we envision for learning about heavy flavours and related PDFs from data at the EIC in the context of what has happened at previous DIS experiments.

I will focus largely on unpolarised proton PDFs from electron(positron)-proton scattering, but also some lower energy and heavy target results.

Possible future interest in broader area, e.g. nuclear PDFs, but not concentrated on here - though many issues common to nucleon and nuclear PDFs in practice.

Inclusive Cross sections and Heavy flavours.

HERAI+II combination data – Neutral Current – Huge Coverage.

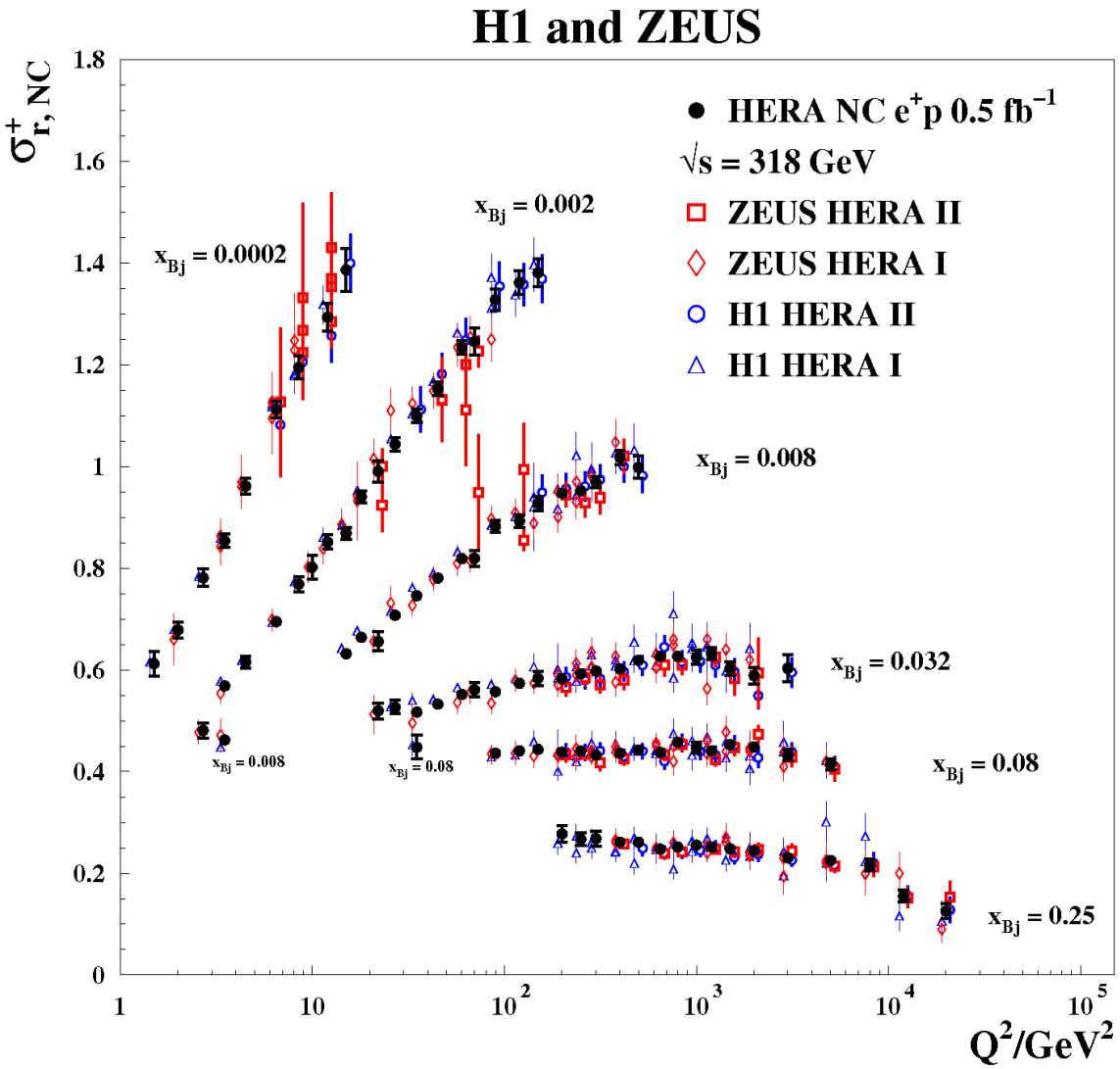

HERAI+II combination data – Charged Current (EPJC 75 (2015) 12, 580).

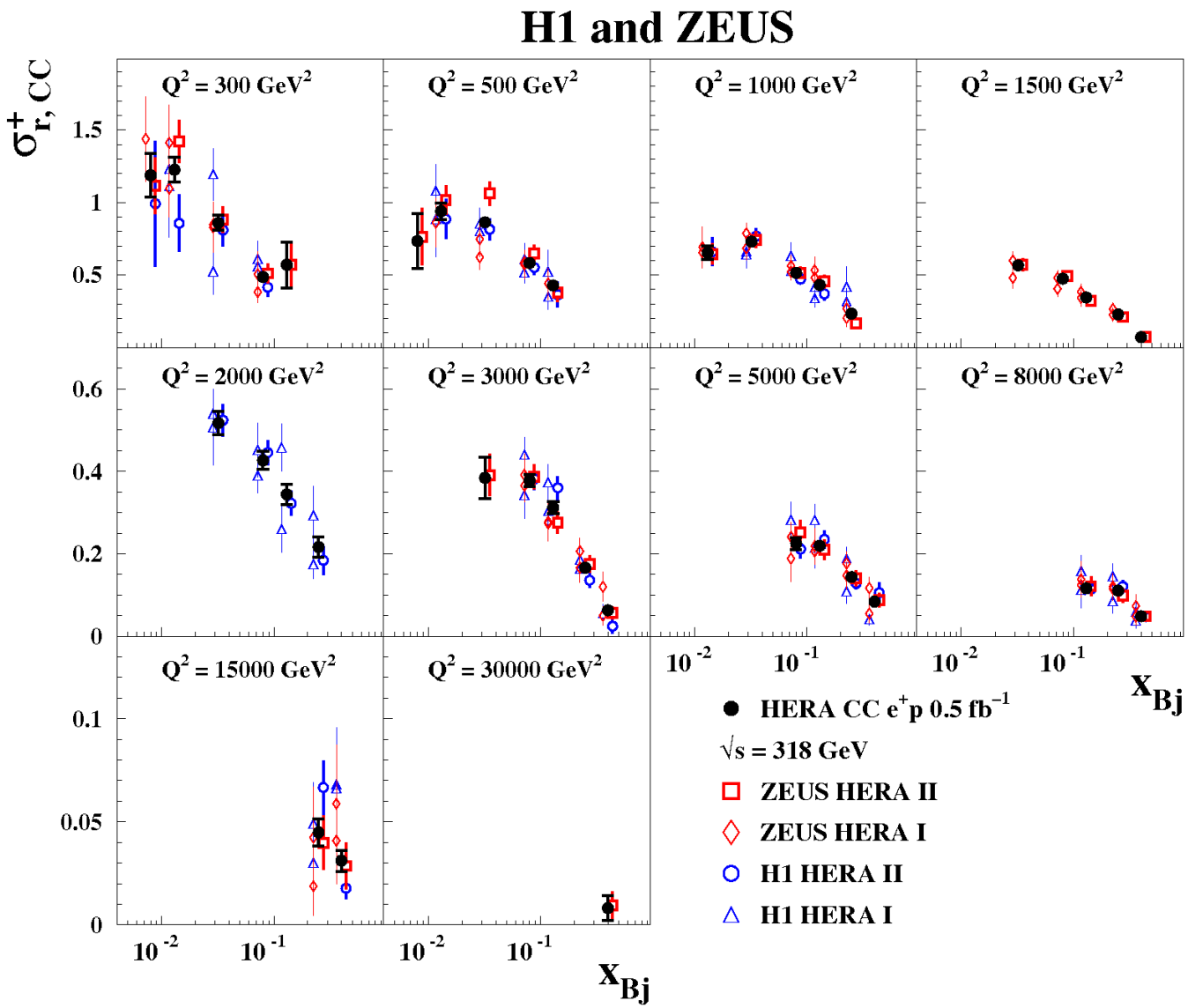

Acts as a major constraint on PDFs, particularly at small x - MSHT.

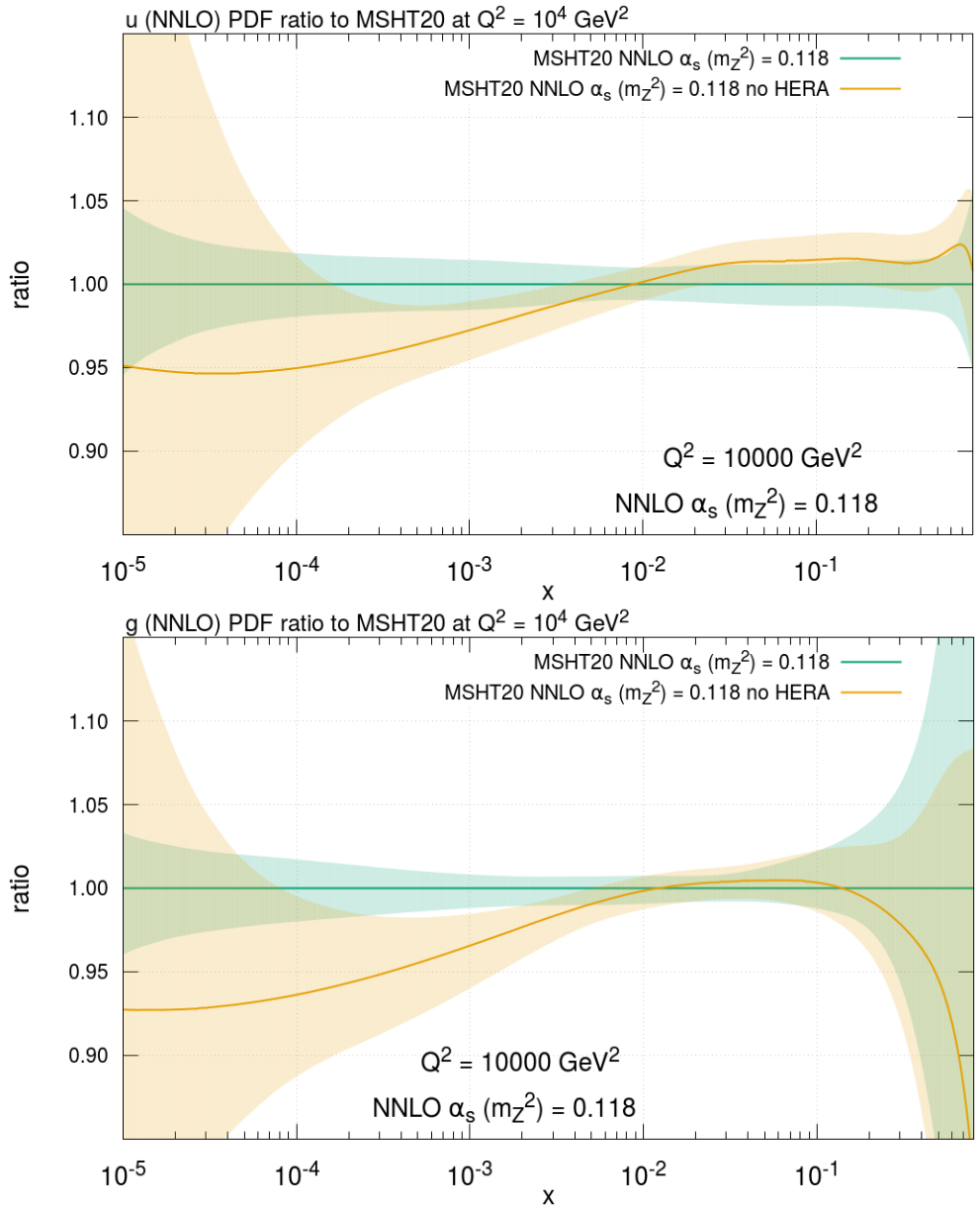

Up to 40% of inclusive cross section is from heavy flavours, mainly charm (EPJC 78 (2018) 6, 473).

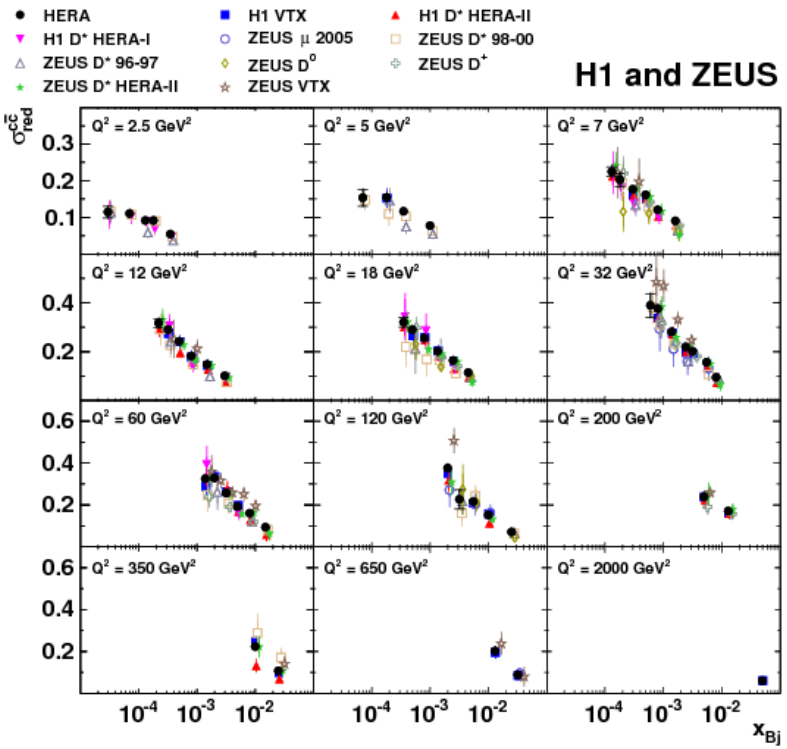

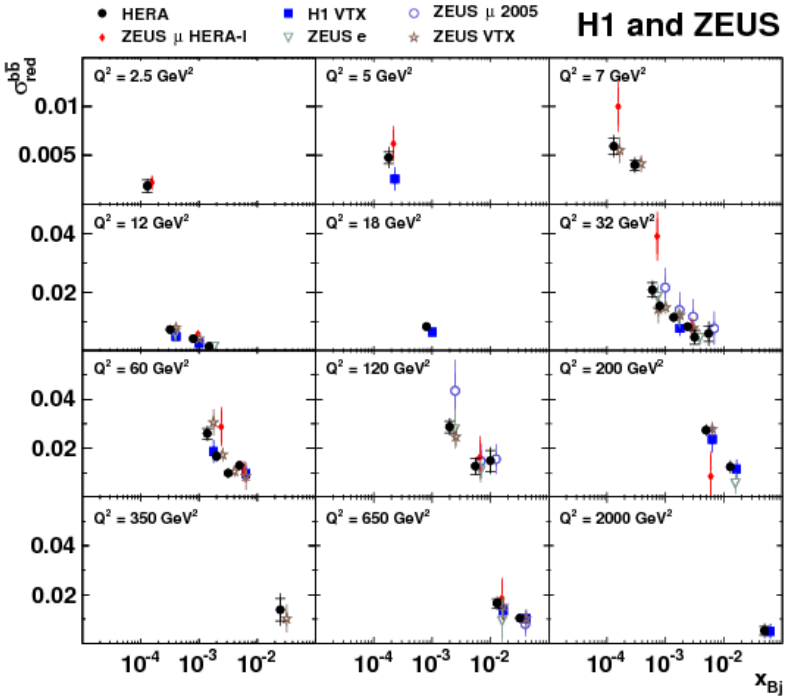

Must fit taking into account contribution to total σ and also directly fit heavy flavour cross section.

Choices for Heavy Flavours in DIS.

Near threshold $Q^2 \sim m_H^2$ massive quarks not partons. Created in final state.

Described using **Fixed Flavour Number Scheme** FFNS (used in ABM(P) and some HERA PDF determinations).

$$F(x,Q^2) = C_k^{FF,n_f}(Q^2/m_H^2) \otimes f_k^{n_f}(Q^2)$$

Does not sum $\alpha_S^n \ln^n Q^2/m_H^2$ terms in perturbative expansion. Usually achieved by definition of heavy flavour parton distributions and solution of evolution equations.

Additional problem FFNS known up to NLO (Laenen *et al.*), but are not fully known at NNLO – $\alpha_S^3 C_{2,Hi}^{FF,3}$ unknown.

Approximations based on some or all of threshold, low-x and high-Q^2 limits can be derived, see Kawamura, *et al.*,, and are sometimes used in fits, e.g. ABM(P) and MMST (at low Q^2). Generally not large except at threshold and very low x.

Variable Flavour - at high scales $Q^2 \gg m_H^2$ heavy quarks behave like massless partons. Sum $\ln(Q^2/m_H^2)$ terms via evolution. **Zero Mass Variable Flavour Number Scheme** (ZM-VFNS). Ignores $\mathcal{O}(m_H^2/Q^2)$ corrections.

$$F(x,Q^2) = C_j^{ZM,n_f} \otimes f_j^{n_f}(Q^2).$$

Partons in different number regions related to each other perturbatively.

$$f_j^{n_f+1}(Q^2) = A_{jk}(Q^2/m_H^2) \otimes f_k^{n_f}(Q^2),$$

Perturbative matrix elements $A_{jk}(Q^2/m_H^2)$ (Buza *et al.*) containing $\ln(Q^2/m_H^2)$ terms relate $f_i^{n_f}(Q^2)$ and $f_i^{n_f+1}(Q^2) \rightarrow$ correct evolution for both.

Can define a **General-Mass Variable Flavour Number Scheme** (VFNS) taking one from the two well-defined limits of $Q^2 \leq m_H^2$ and $Q^2 \gg m_H^2$.

Variants used in CT, HERA, MSHT, NNPDF fits. Different versions converge at higher orders.

At NLO the partons remain continuous if transition point is taken as $Q^2 = m_H^2$. ZM-VFNS possible, if inaccurate.

At NNLO lead to discontinuities in partons.

Heavy flavour no longer turns on from zero at $\mu^2 = m_c^2$

$$(c + \bar{c})(x, m_c^2) = A_{Hg}^2(m_c^2) \otimes g(m_c^2)$$

In practice turns on from negative value, (for general gluon).

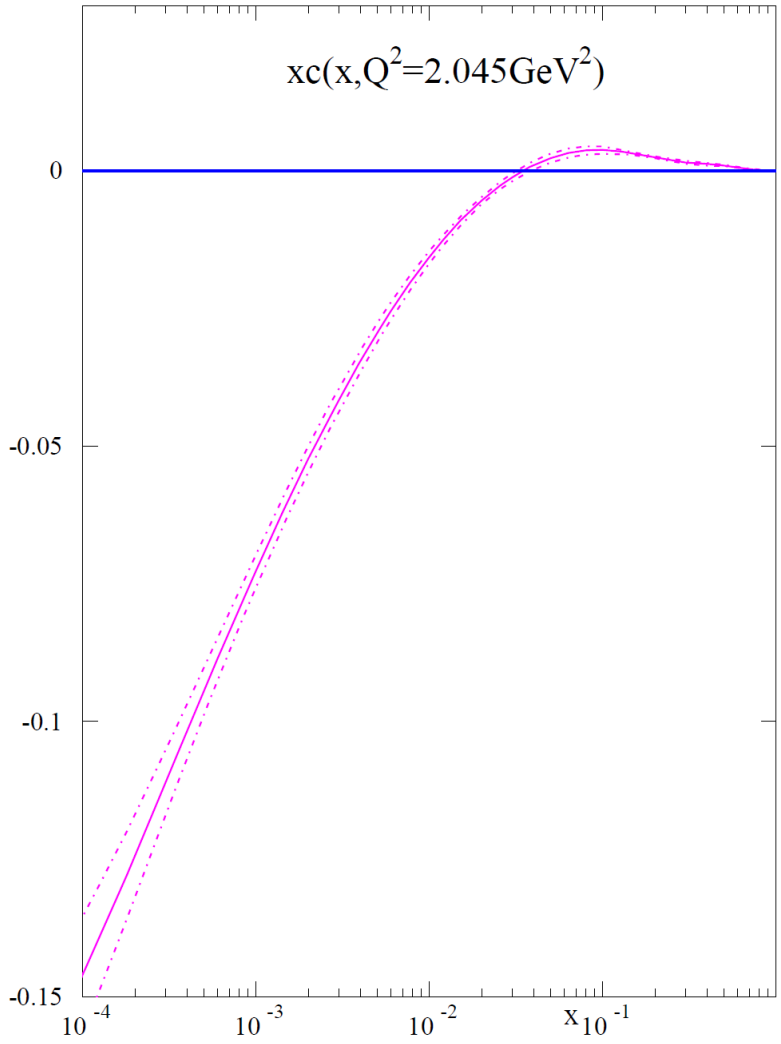

Higher orders

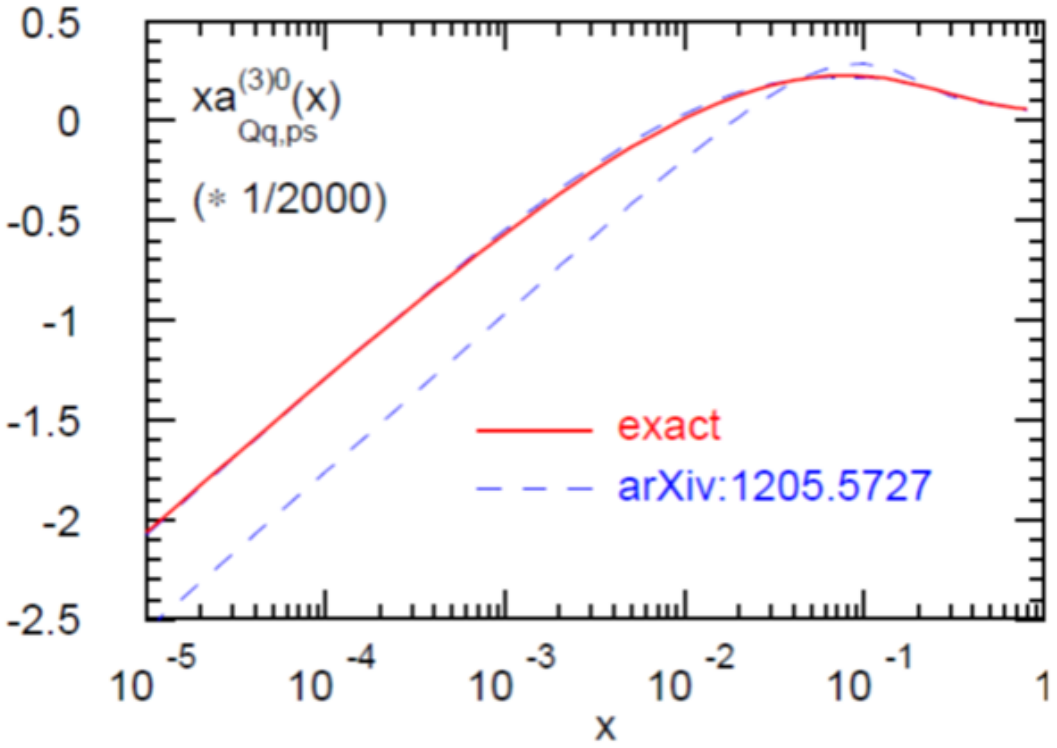

At $\mathcal{O}(\alpha_S^3)$ similar form seemingly, but A_{Hg} not yet fully known.

Calculation of matrix elements part of an enormous project by Blümlein et al. e.g (Nucl.Phys.B 890 (2014) 48-151).

Goes into NNLO FFNS coefficient functions.

Difference between FFNS and GM-VFNS

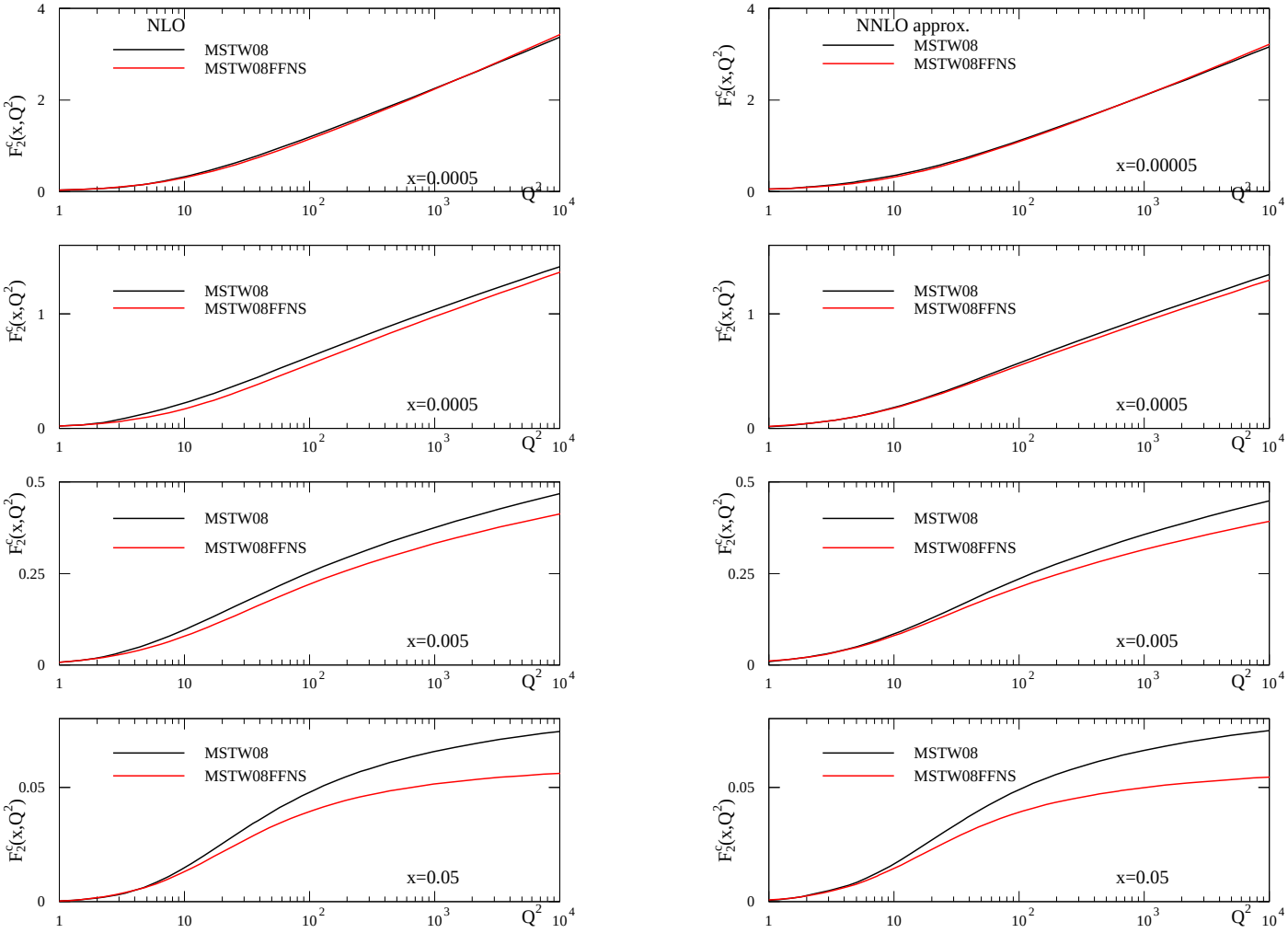

At higher Q^2 charm structure function for FFNS nearly always lower than any GM-VFNS. NNLO uses $\mathcal{O}(\alpha_S^2)$ coefficient functions for $F_2^c(x, Q^2)$.

Differences can be significant in full inclusive structure function $F_2(x, Q^2)$ (EPJC 74 (2014) 7, 2958).

However differences biggest in high-Q^2 regime.

Not obviously too important for EIC, or in fact, so much for $\sigma^{c\bar{c}}(x, Q^2)$ at HERA.

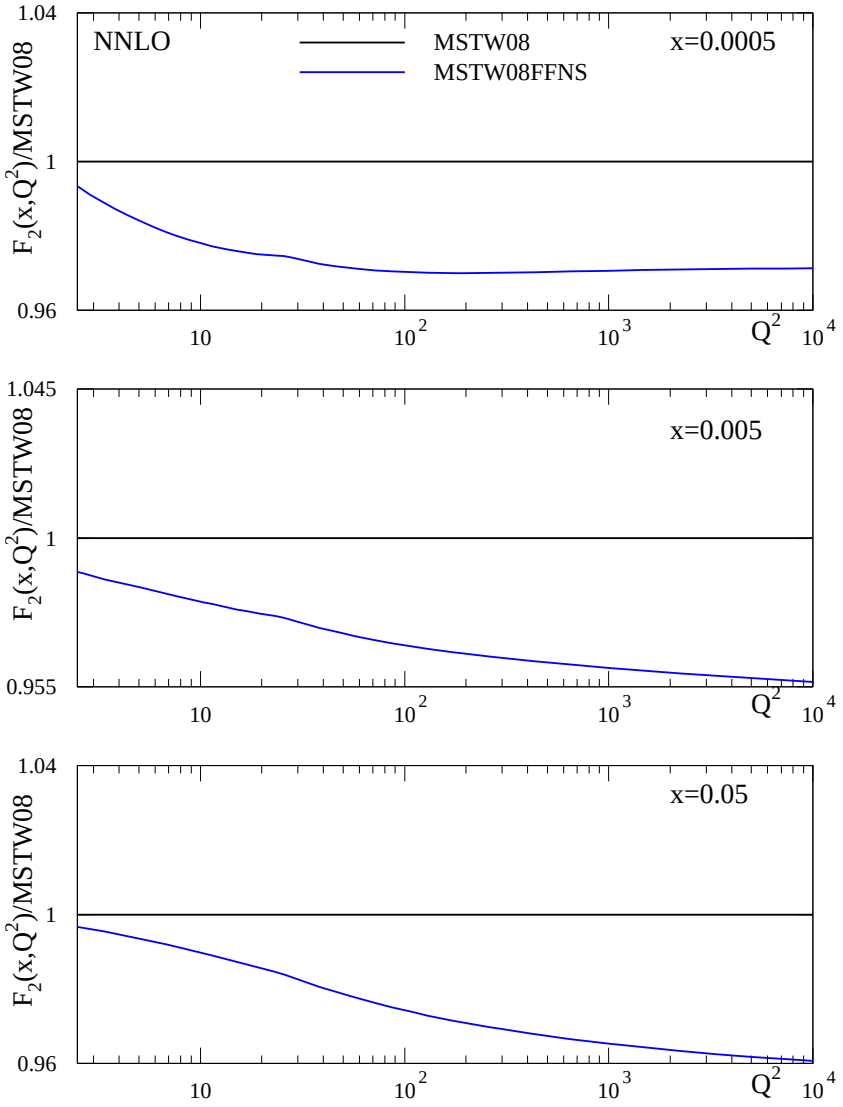

Longitidudinal Structure Function

Directly related to gluon. Significant potentially at high inelasticity y.

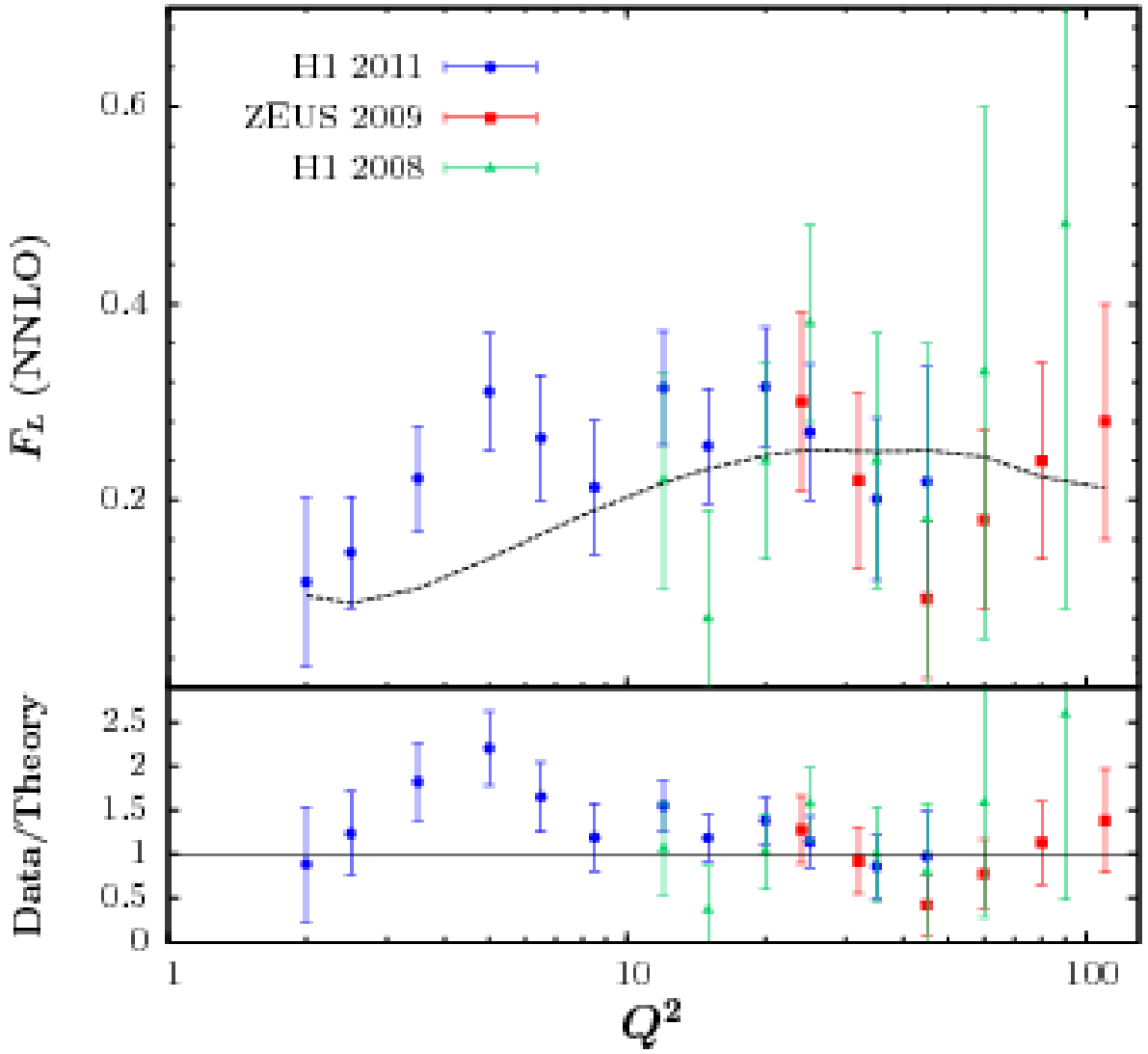

The heavy flavour contribution is supressed near threshold.

Cross section $\sim v^3$ for velocity of heavy quark in centre of mass frame.

Compare with $\sim v$ for $F_2(x, Q^2)$.

However, still some regions where significant at the EIC.

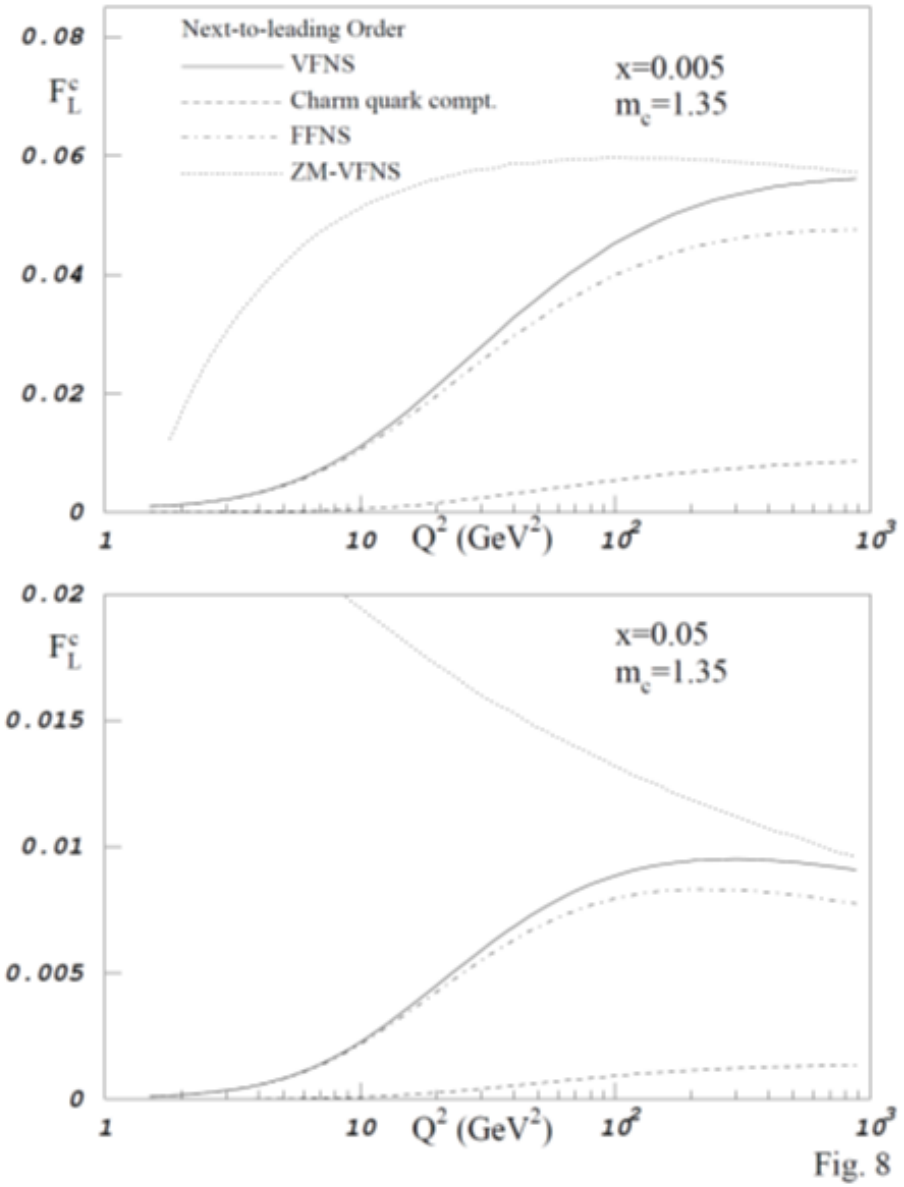

Fig. 8

EIC kinematic range compared to HERA (plot from Y. Furletova).

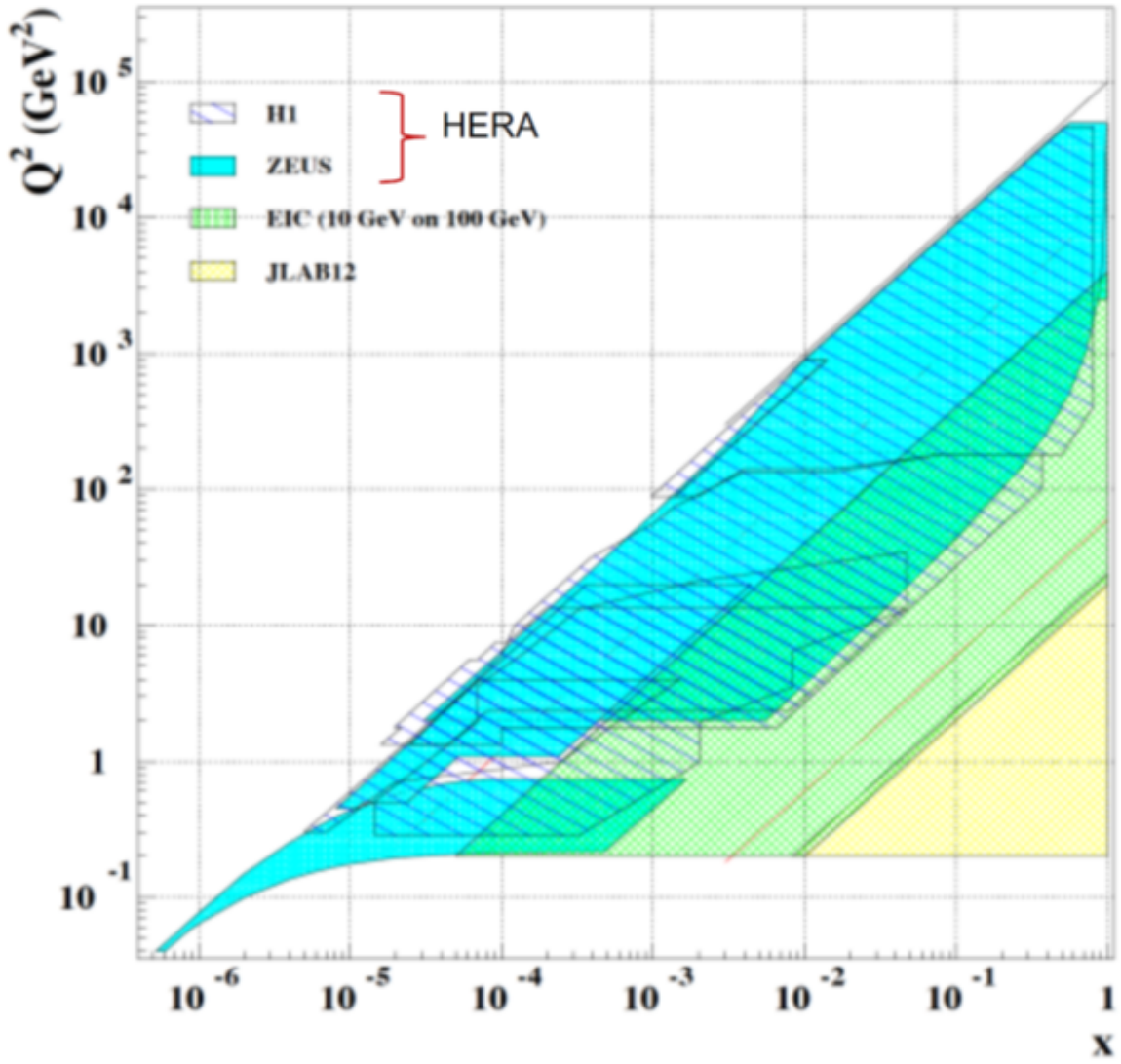

Some overlap. EIC clearly generally at higher x lower Q^2.

Projection for possible EIC heavy flavour data.

- Inclusive eA scattering measurements

arXiv:1708.01527

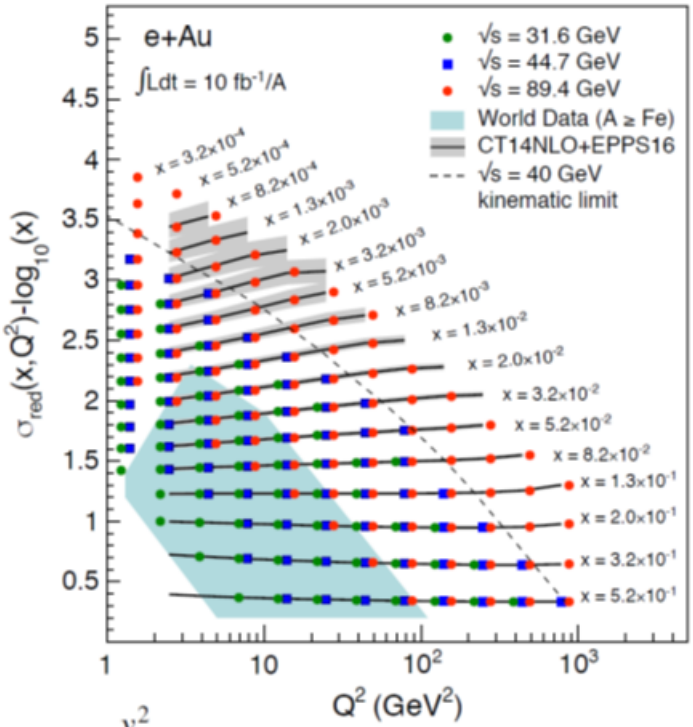

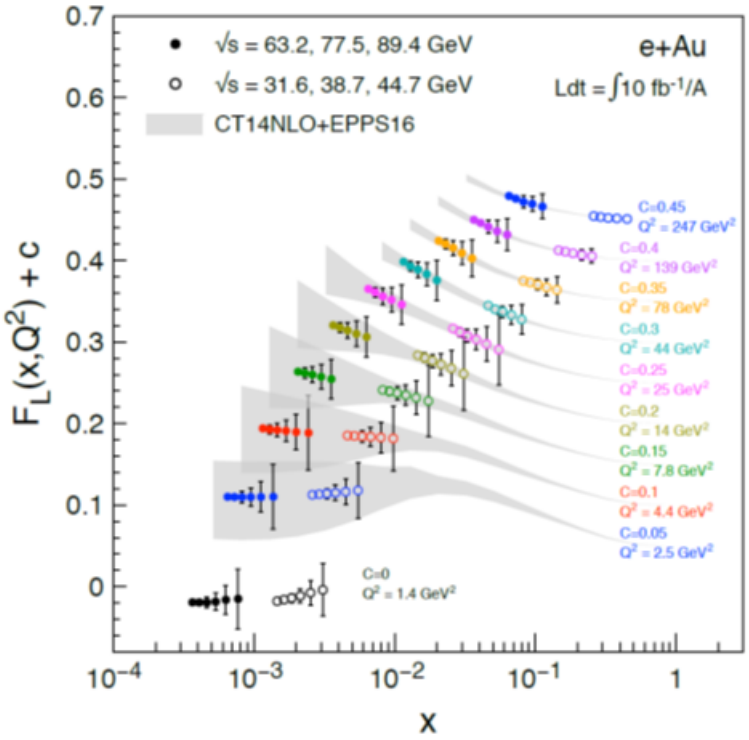

$$\sigma_{\text{red}} = F_2 - \frac{y^2}{Y_+} F_L$$

$$\left(\frac{d^2\sigma}{dxdQ^2}\right) = \frac{2\pi\alpha^2 Y_+}{xQ^4}\left(F_2 - \frac{y^2}{Y_+}F_L\right)$$

ABM charm fit (1909.03533)

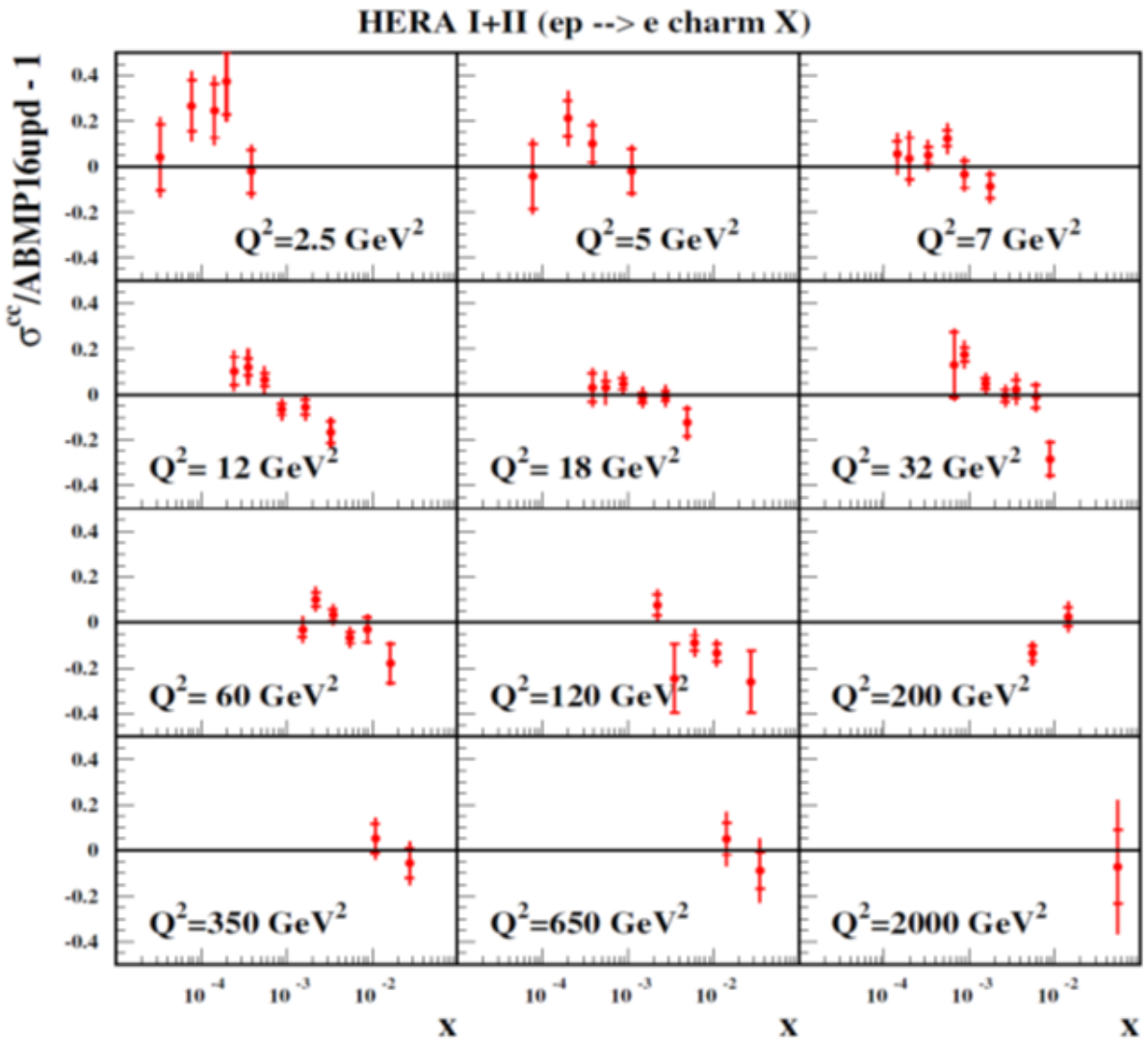

Fit not bad, but slope with x not steep enough at low x, Q^2.

MSHT heavy flavour fit

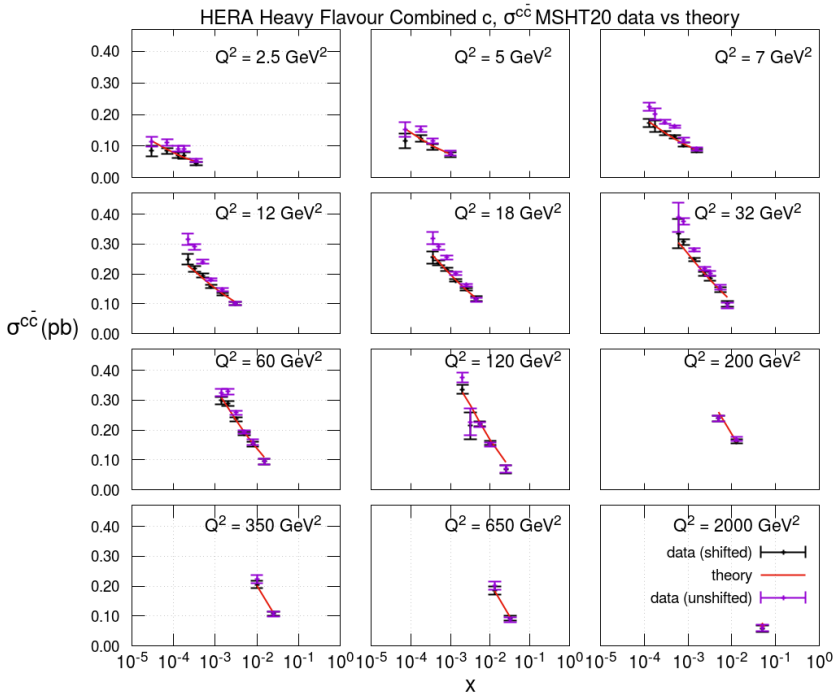

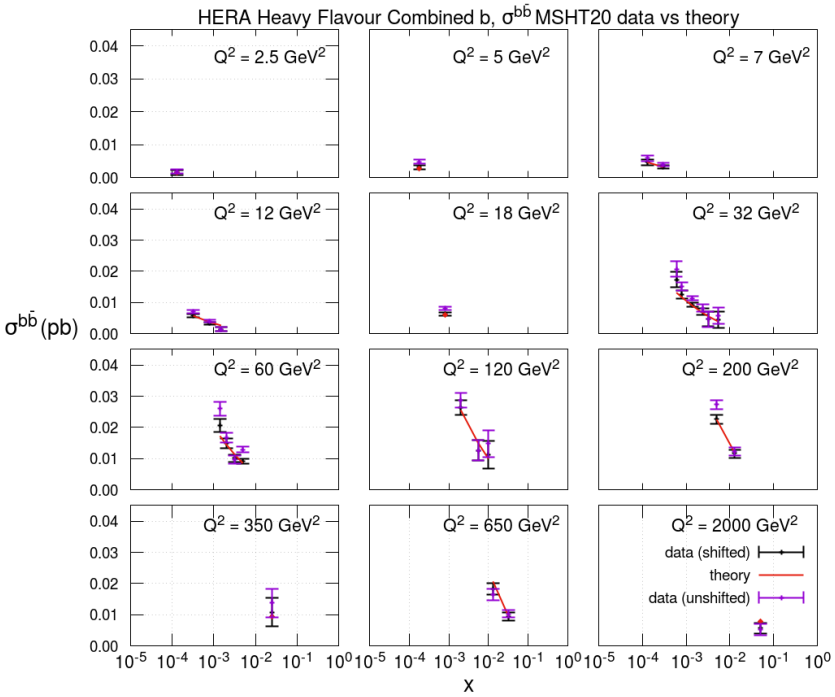

Similar issue with fit, total $\chi^2 \approx 130/79$. Similar in other fits and comparisons, not really a FFNS – GMVFNS difference.

Tensions between inclusive structure function data and heavy flavour.

Latter prefers steeper gluon – (EPJC 78 (2018) 6, 473).

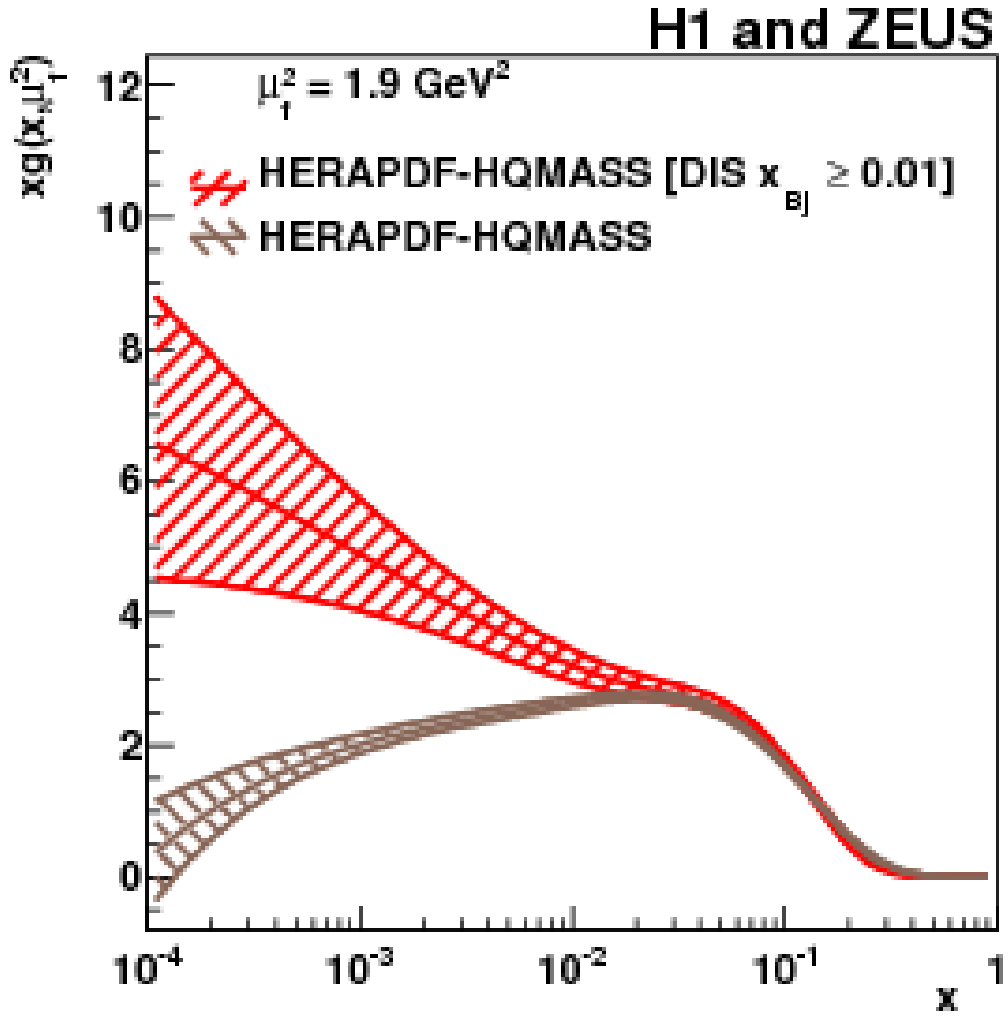

The EIC will get into this range where tension is seen.

Mass determination

By Fitting HERA data can determine heavy quark masses quite well.

HERA results – (EPJC 78 (2018) 6, 473)

$$m_c(m_c) = 1.290^{+0.046}_{-0.041}(\text{exp/fit})^{+0.062}_{-0.014}(\text{model})^{+0.003}_{-0.031}(\text{parameterisation})\ \text{GeV},$$
$$m_b(m_b) = 4.049^{+0.104}_{-0.109}(\text{exp/fit})^{+0.090}_{-0.032}(\text{model})^{+0.001}_{-0.031}(\text{parameterisation})\ \text{GeV}.$$

ABMP results – (PRD 96 (2017) 1, 014011)

$$m_c(m_c) = 1.252 \pm 0.018\ \text{GeV},$$
$$m_b(m_b) = 3.84 \pm 0.12\ \text{GeV},$$
$$m_t(m_t) = 160.9 \pm 1.1\ \text{GeV},$$

Both determined using FFNS with masses defined in $\overline{MS}$ mass renormalization scheme. Good agreement.

Can also use pole mass scheme.

Transformation bewteen the two (PDG)

$$m_Q = \overline{m}_Q(\overline{m}_Q)\Bigg\{1 + \frac{4\overline{\alpha}_s(\overline{m}_Q)}{3\pi} + \left[-1.0414\sum_q\left(1 - \frac{4}{3}\frac{\overline{m}_q}{\overline{m}_Q}\right) + 13.4434\right]\left[\frac{\overline{\alpha}_s(\overline{m}_Q)}{\pi}\right]^2 + \left[0.6527N_L^2 - 26.655N_L + 190.595\right]\left[\frac{\overline{\alpha}_s(\overline{m}_Q)}{\pi}\right]^3\Bigg\},$$

For the bottom-quark mass is $(1 + 0.095 + 0.045 + 0.036)$ and for charm is $(1 + 0.16 + 0.14 + 0.18)$.

i.e. For bottom quark mass factor $M_b^{\rm pole} = \bar{M}_b(\bar{M}_b) * 1.175 + \mathcal{O}(0.15\ {\rm GeV})$

while for the charm quark no real convergence at all.

However, $M_b^{\rm pole} - M_c^{\rm pole} = 3.4\ {\rm GeV}$ to good accuracy (Hoang, Manohar).

MSHT find $M_c^{\rm pole} \sim 1.4\ {\rm GeV}$ and $M_b^{\rm pole} \sim 4.8\ {\rm GeV}$

The EIC – low Q^2, W^2 and Higher Twist.

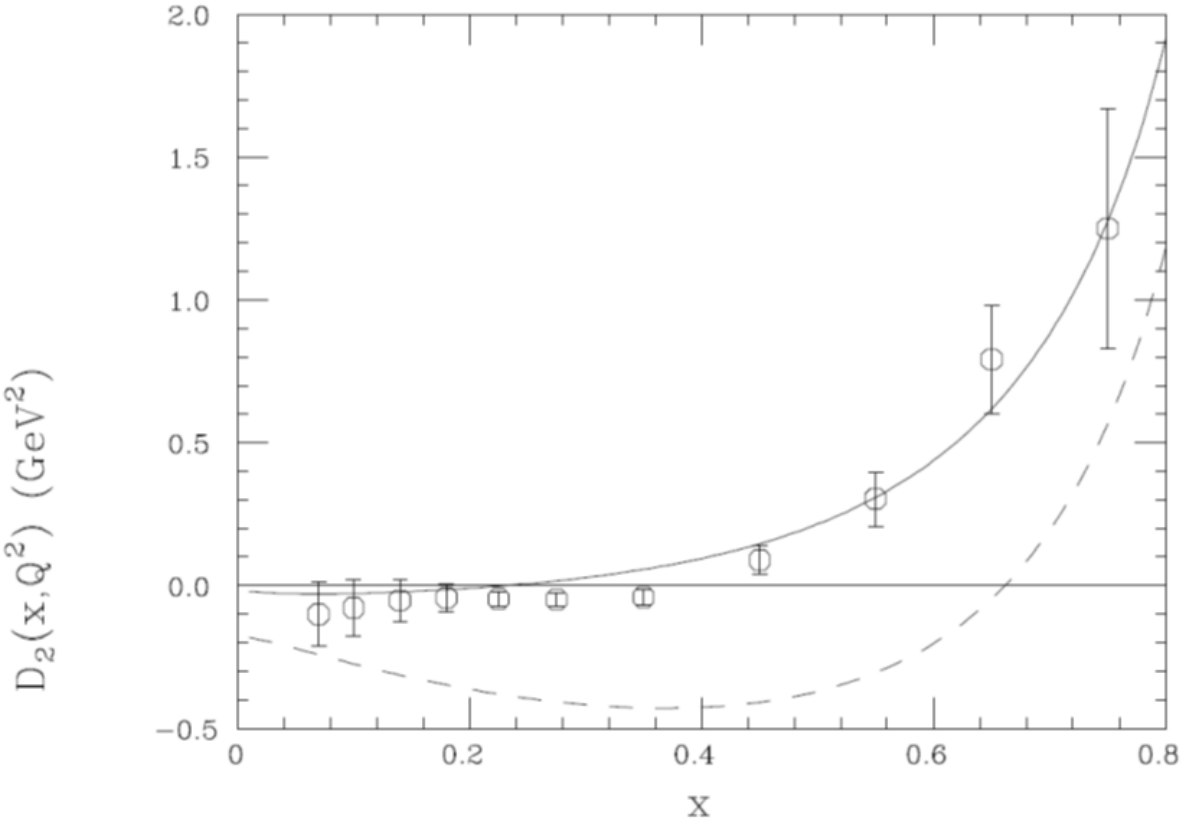

Large at large x (low W^2), but protected in $F_2(x, Q^2)$ (but not $F_3(x, Q^2)$) from Adler sum rule – renormalon calculation Dasgupta and Webber.

Results obtained from fitting low Q^2 and W^2 data, ABMP left and RT right.

	$H_2^{\tau=4}(x)/\mathrm{GeV}^2$	$H_T^{\tau=4}(x)/\mathrm{GeV}^2$
$x = 0.0$	0.023 ± 0.019	-0.319 ± 0.126
$x = 0.1$	-0.032 ± 0.013	-0.134 ± 0.040
$x = 0.3$	-0.005 ± 0.009	-0.052 ± 0.030
$x = 0.5$	0.025 ± 0.006	0.071 ± 0.025
$x = 0.7$	0.051 ± 0.005	0.030 ± 0.012
$x = 0.9$	0.003 ± 0.004	0.003 ± 0.007
$x = 1$	0	0

x	NLO	NNLO	NLO FFNS	NNLO FFNS
0–0.0005	0.13	0.38	0.35	0.47
0.0005–0.005	0.05	0.35	0.25	0.41
0.005–0.01	−0.11	0.13	−0.01	0.14
0.01–0.06	−0.15	−0.04	−0.10	−0.10
0.06–0.1	0.08	0.01	0.07	0.05
0.1–0.2	−0.12	−0.07	−0.15	−0.12
0.2–0.3	−0.16	−0.11	−0.21	−0.16
0.3–0.4	−0.20	−0.16	−0.23	−0.17
0.4–0.5	−0.09	−0.09	−0.10	−0.05
0.5–0.6	0.39	0.28	0.39	0.39
0.6–0.7	1.8	1.4	1.9	1.7
0.7–0.8	6.5	5.0	7.0	6.2
0.8–0.9	15.0	9.9	18.0	15.2

Table 3: The values of the higher-twist coefficients D_i of (16), in the chosen bins of x, extracted from the NLO and NNLO GM-VFNS global fits and the NLO and NNLO FFNS fits to DIS data.

Similar until extremely high x (where target mass treatment different).

Fits well with previous renormalon expectations.

Intrinsic charm

Formally of higher twist, i.e. $\mathcal{O}(\Lambda^2/m_c^2)$.

Proposed that it could be enhanced at high x by Brodsky et al in 1983.

$$\hat{c}(x) = Ax^2[6x(1+x)\ln x + (1-x)(1+10x+x^2)]$$

Possible enhancement at high-x, similar to the large higher twist expected at low W^2.

Therefore no expected constraint from HERA data.

Potentially of relevance for EIC data.

Investigations in PDF fits

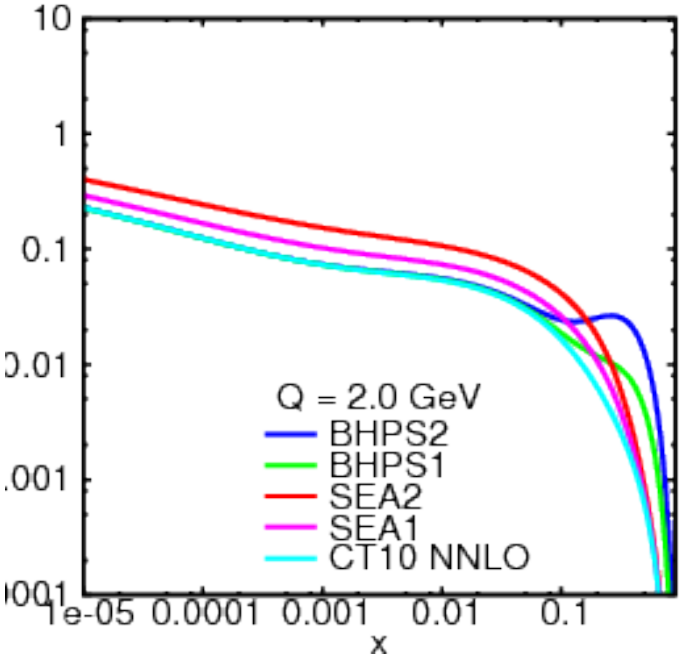

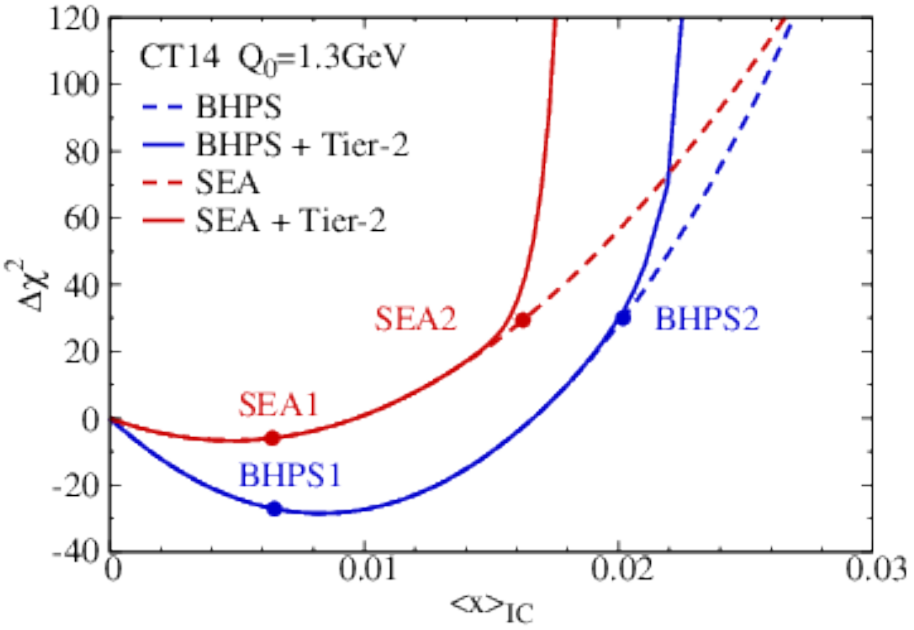

CT add this type of intrinsic charm model, and sea quark type intrinsic charm, and see the effect on global fits. Some limited evidence for preference, e.g JHEP 02 (2018) 059.

NNPDF recently started including "fitted charm" (not identical to "intrinsic charm") as their default, e.g. EPJC 76 (2016) 11, 647.

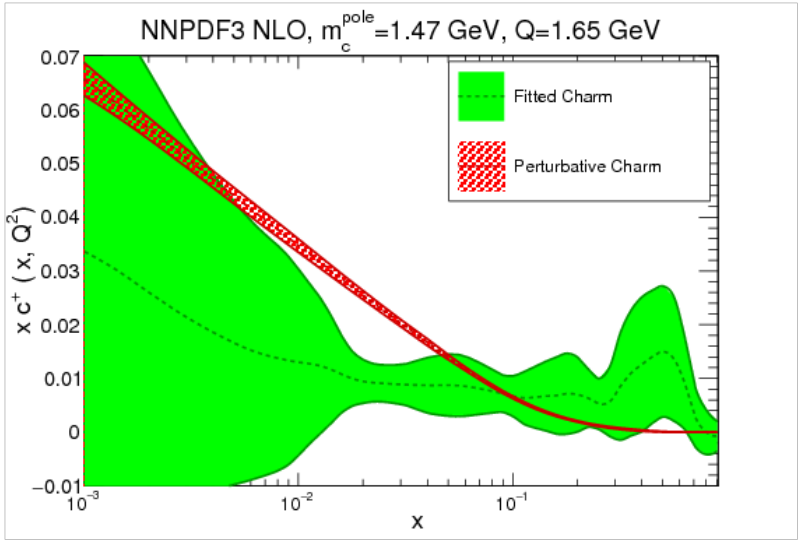

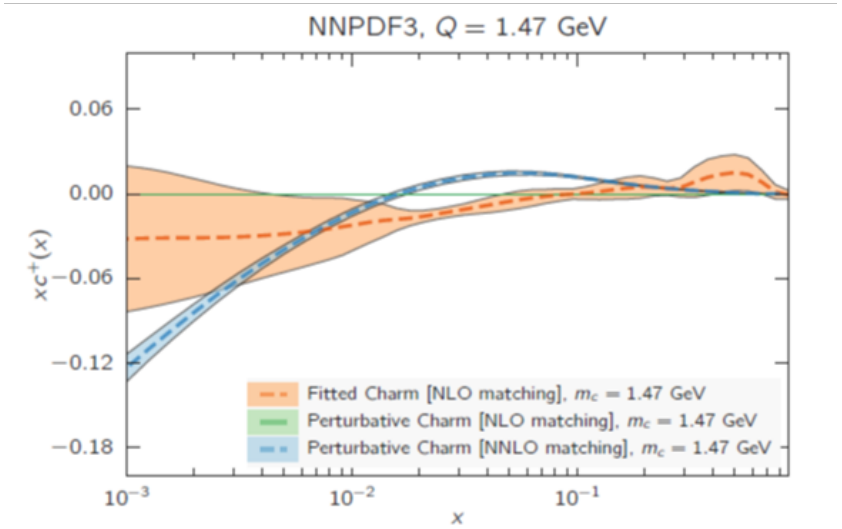

Very different to perturbative only charm, with much bigger uncertainty.

Larger than perturbative charm at highest x but smaller for $x \sim 0.01$.

Also very different to CT instrinsic charm models.

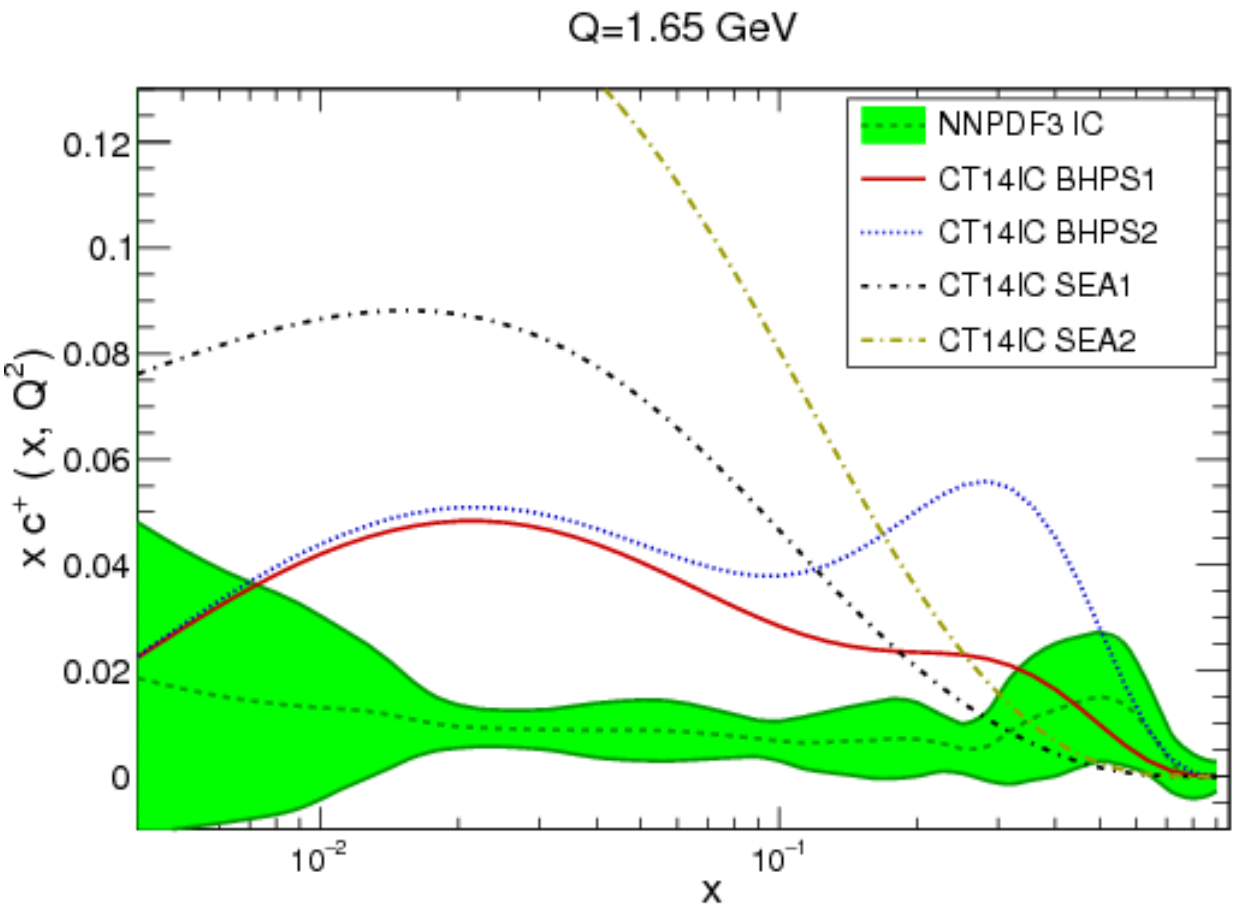

Tends to be lower that perturbative charm at lowish x.

Possibility of $A_{H,g(q)}$ terms in transition matrix.

Really higher order theory correction?

In some NNPDF fits try fitting old EMC data (NPB 213 (1983) 31-64).

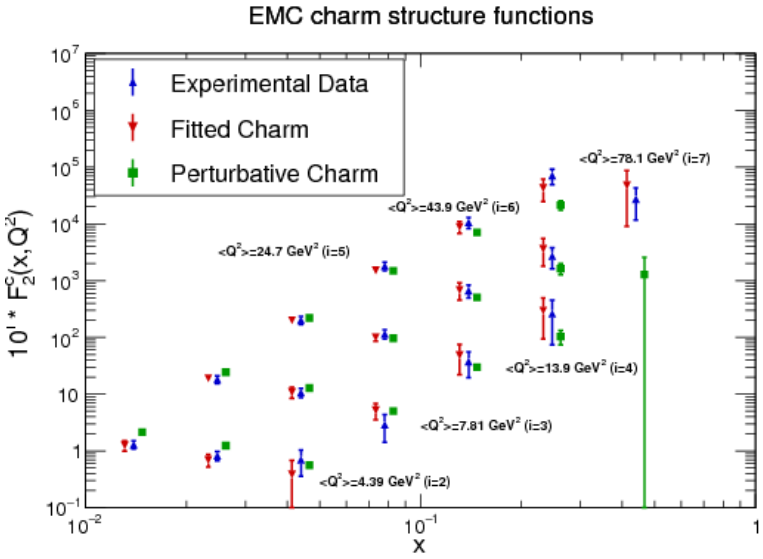

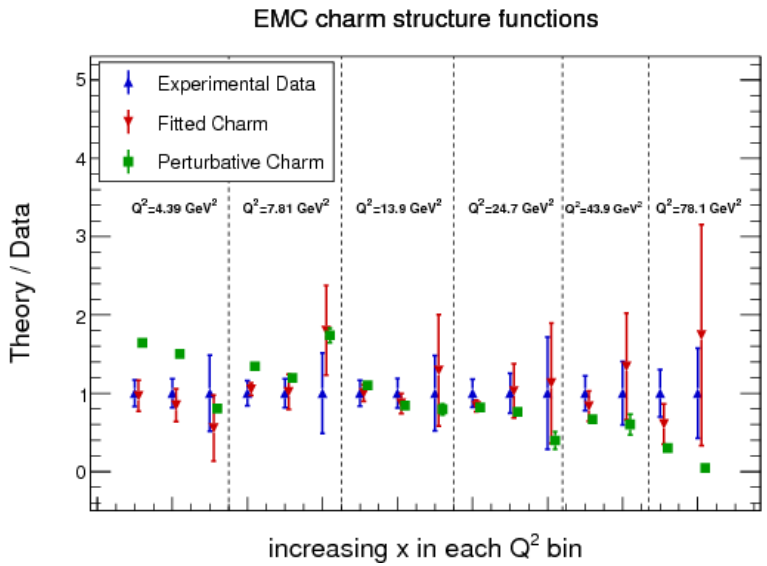

Clearly prefers supression at smaller x, and also some enhancement as $x \to 1$.

Consistent with suggestions from LHC data sensitive to flavours (W, Z).

Note however, EMC data relied on large corrections using LO theory generators and extremely basic PDFs. Significant question mark.

MSTW tried fitting EMC data. Overshoot lower x data even at NLO with dynamical charm.

High-x intrinsic charm with modified coefficient functions, $m_c^2 \rightarrow m_c^2 + \Lambda^2$, at threshold works ok.

At low Q^2 and W^2 we likely need to worry about nonperturbative or higher twist effects beyond just that of intrinsic charm.

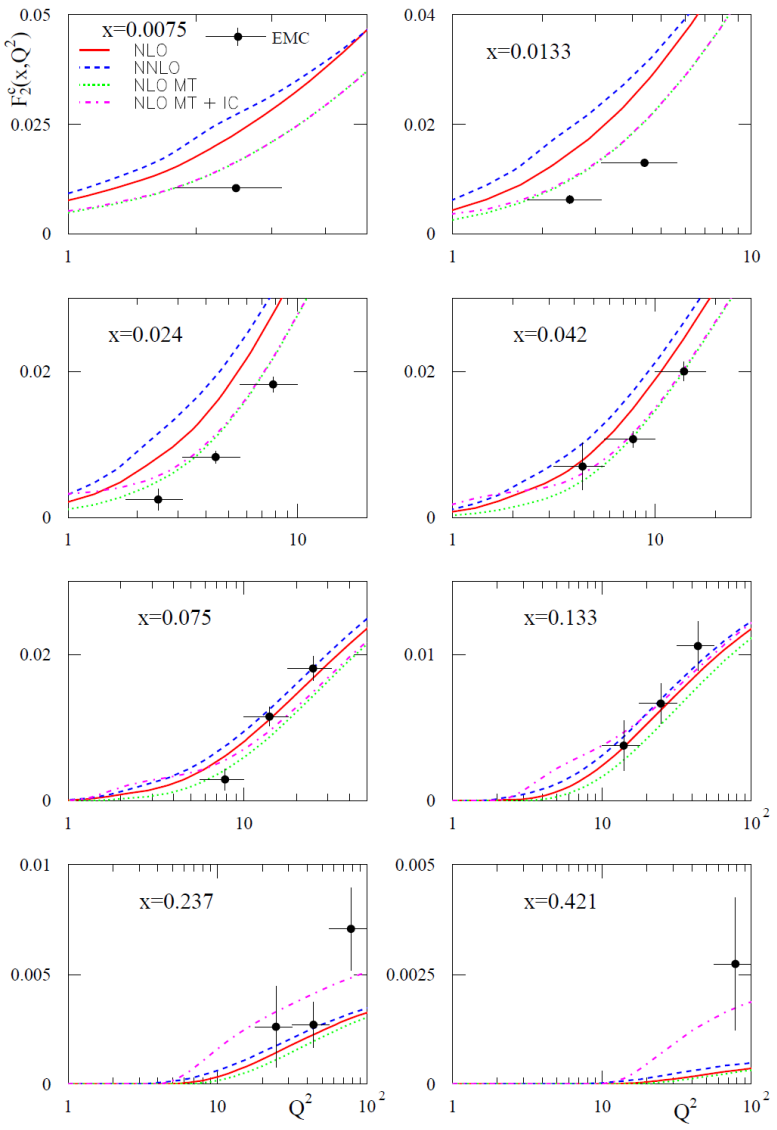

Figure 39: The comparison of the EMC charm data [165] to our predictions at NLO and NNLO. MT stands for the modified threshold approach and IC stands for inclusion of intrinsic charm.

Intrinsic charm and a GM-VFNS.

Strictly speaking ambiguity in individual coefficient functions in GM-VFNS, which vanishes at all orders for only dynamical heavy flavour, is $\mathcal{O}(m_c^2/Q^2)$.

Coupled with magnitude of intrinsic charm, i.e. $\mathcal{O}(\Lambda^2/m_c^2)$ leads to an uncertainty/error of cross sections from intrinsic charm of $\mathcal{O}(\Lambda^2/Q^2)$, i.e. of standard higher twist corrections.

May be significant if intrinsic charm enhanced in some region, e.g. high-x, i.e. region of large higher twist effects to inclusive cross section.

Unsure about inclusion of significant component of higher twist away from high x.

Charged Current Charm production

Long existing measurements of dimuon production in neutrino DIS on heavy targets CCFR, NuTeV, (Phys.Rev.D 74 (2006) 012008).

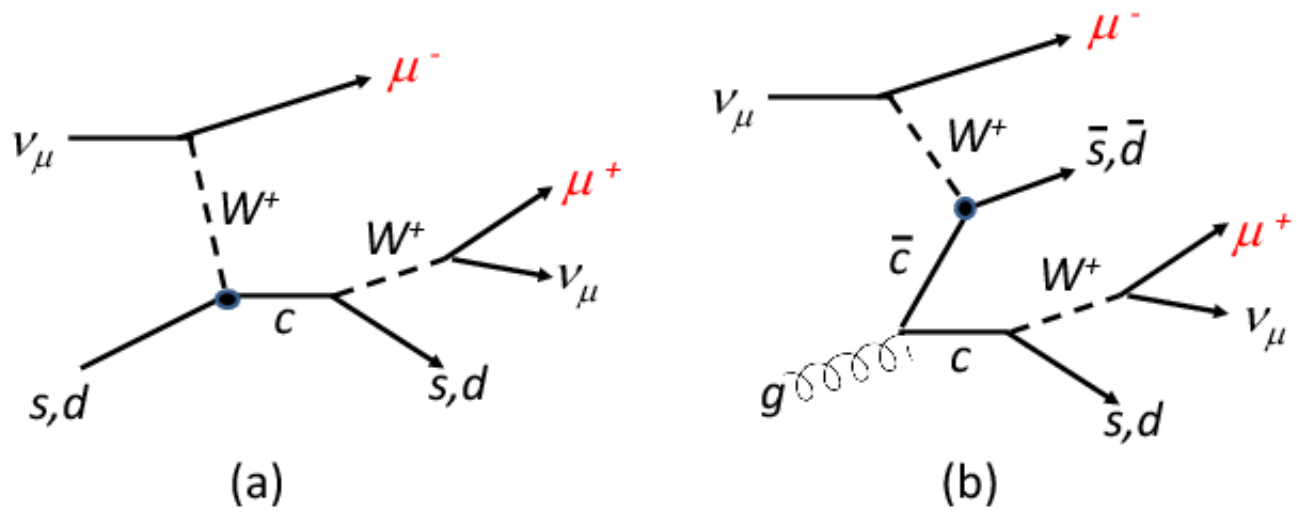

Dominated by strange (anti)quark initial state - traditionally main constraint on strangeness.

Measurements using both ν_μ and $\bar{\nu}_\mu$ beams at different energies.

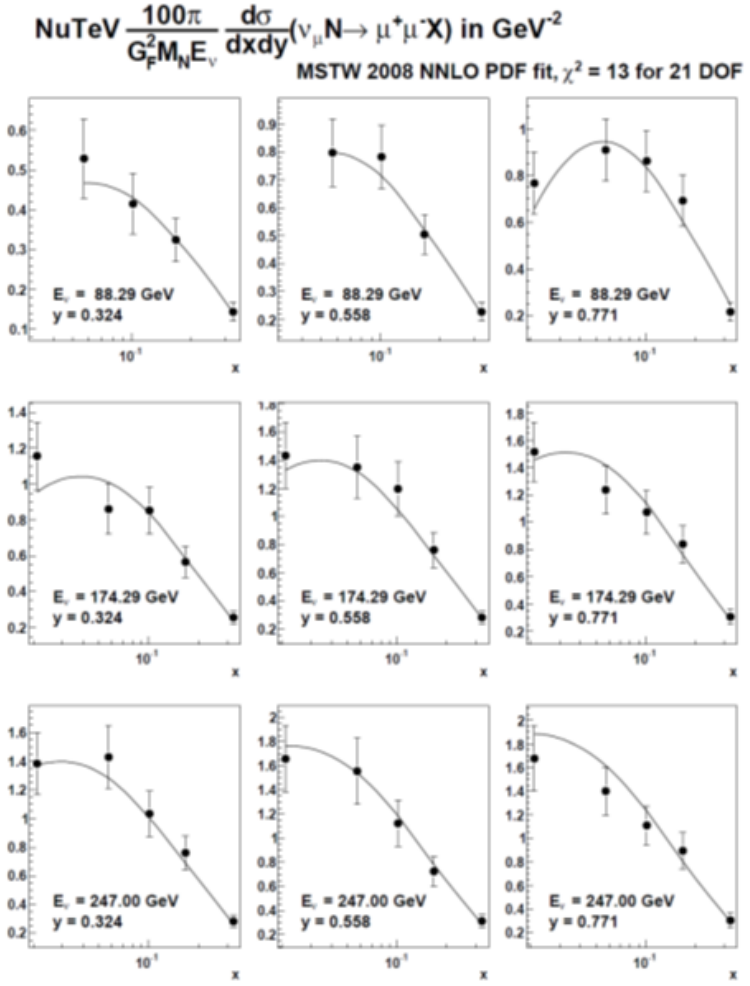

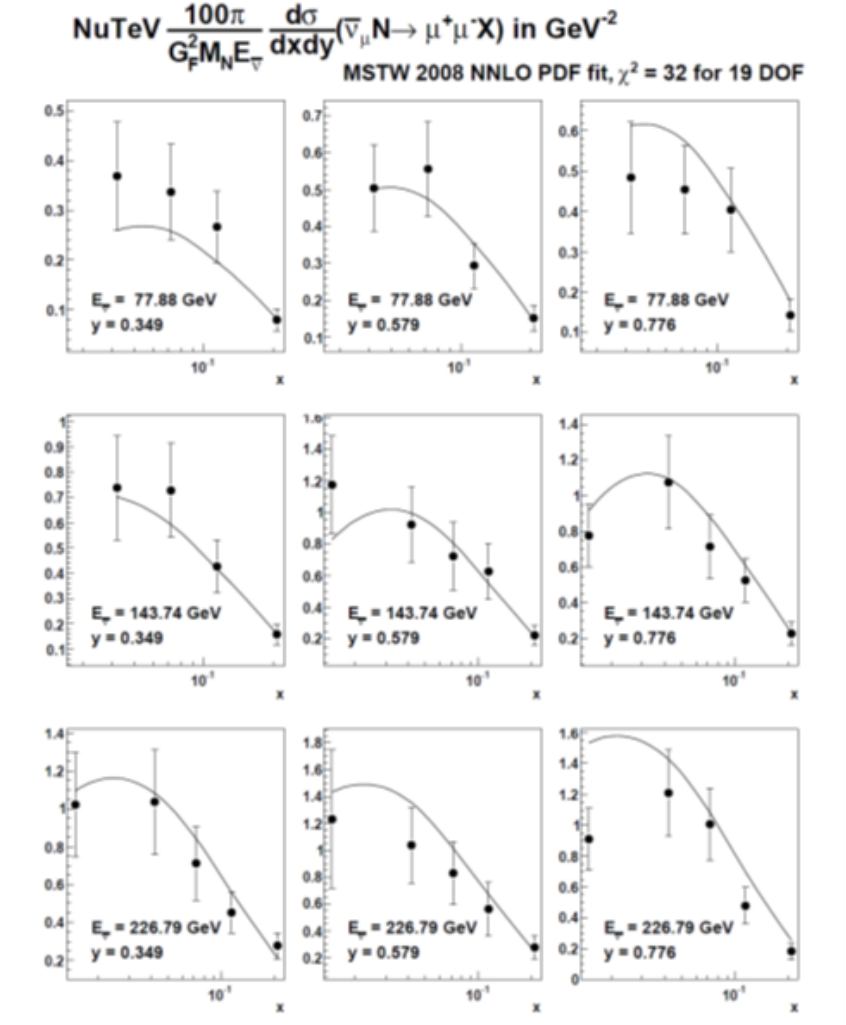

Gives constraint on total strangeness, implied supression by $\sim 50\%$ compared to light quarks at low Q^2 and on strangeness asymmetry.

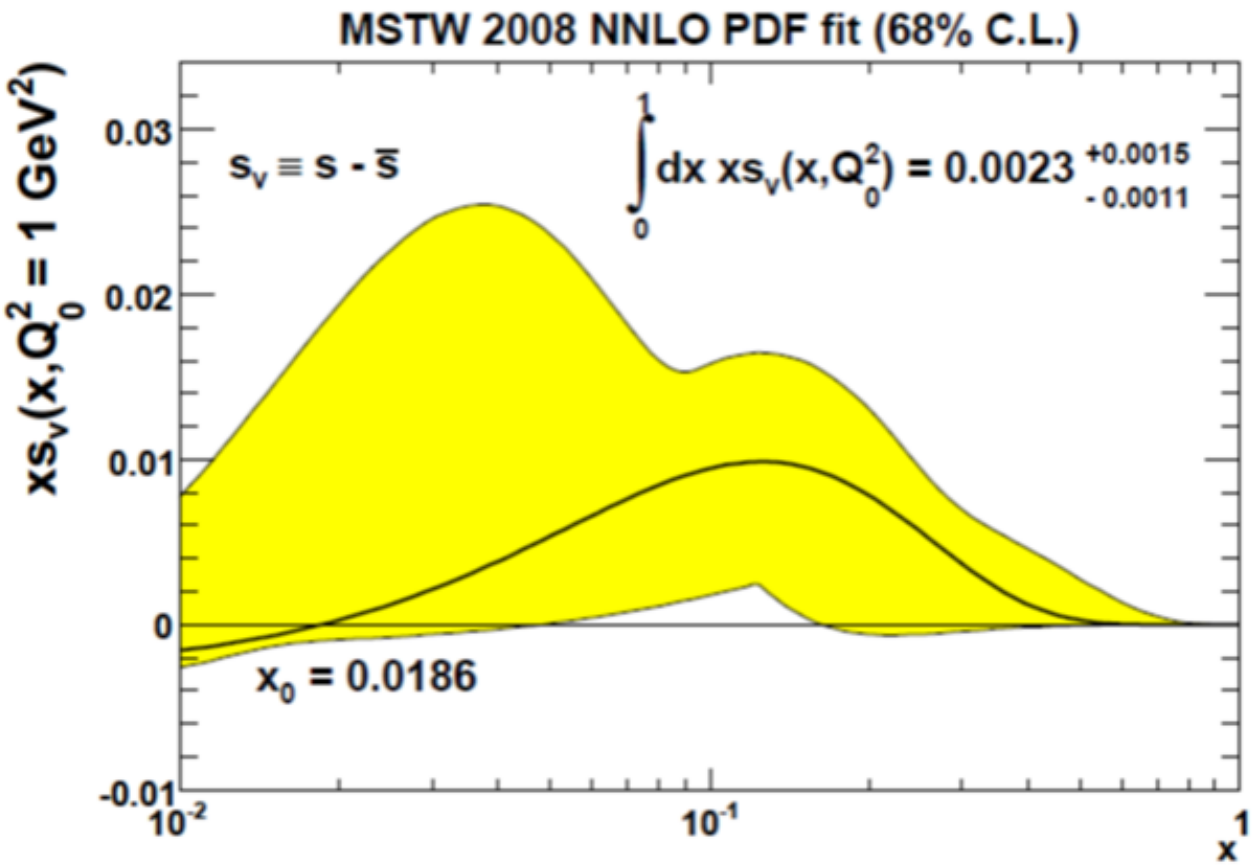

Two major issues – until recently only at NLO and recent ATLAS data on W, Z in tension.

Inclusion of new NNLO corrections.

NNLO corrections to dimuon production (Phys. Rev. Lett. 116 (2016), Berger *et al.*, J. Gao, arXiv:1710.04258).

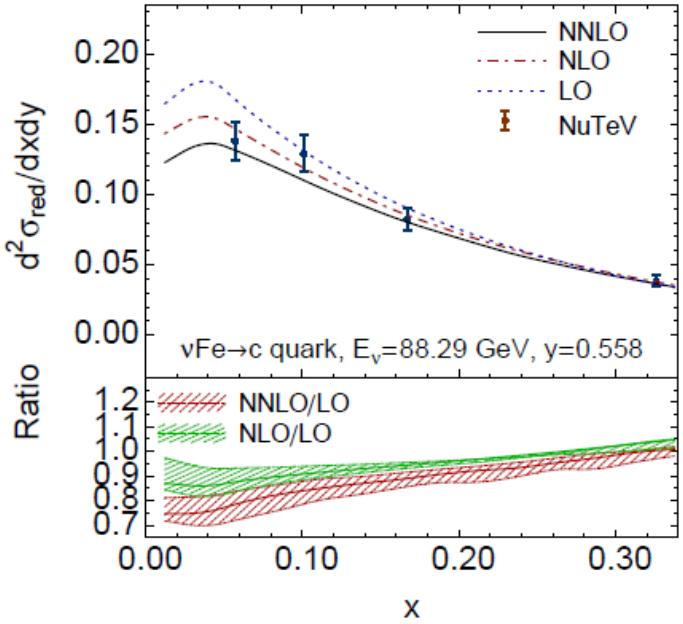

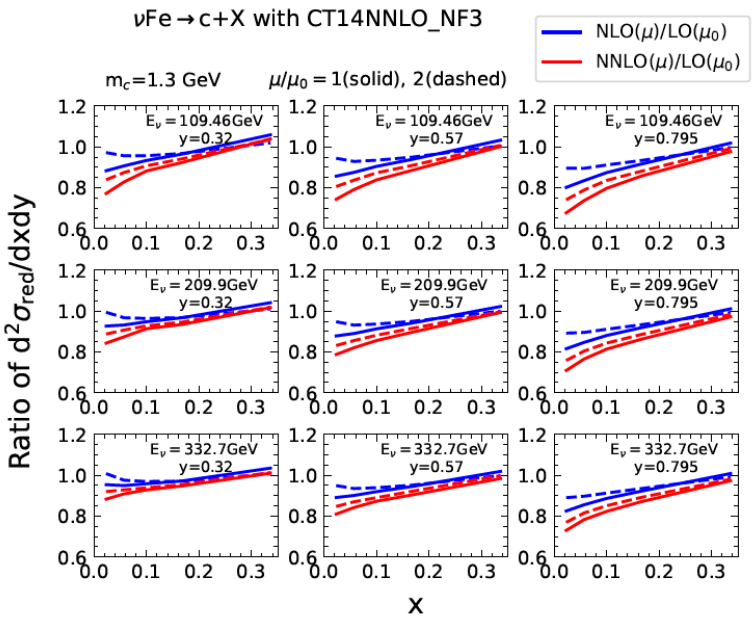

NNLO correction negative, but larger in size at lower x

Impacts on tension between dimuon data and LHC W, Z data.

Extremely high precision data on W, Z from ATLAS

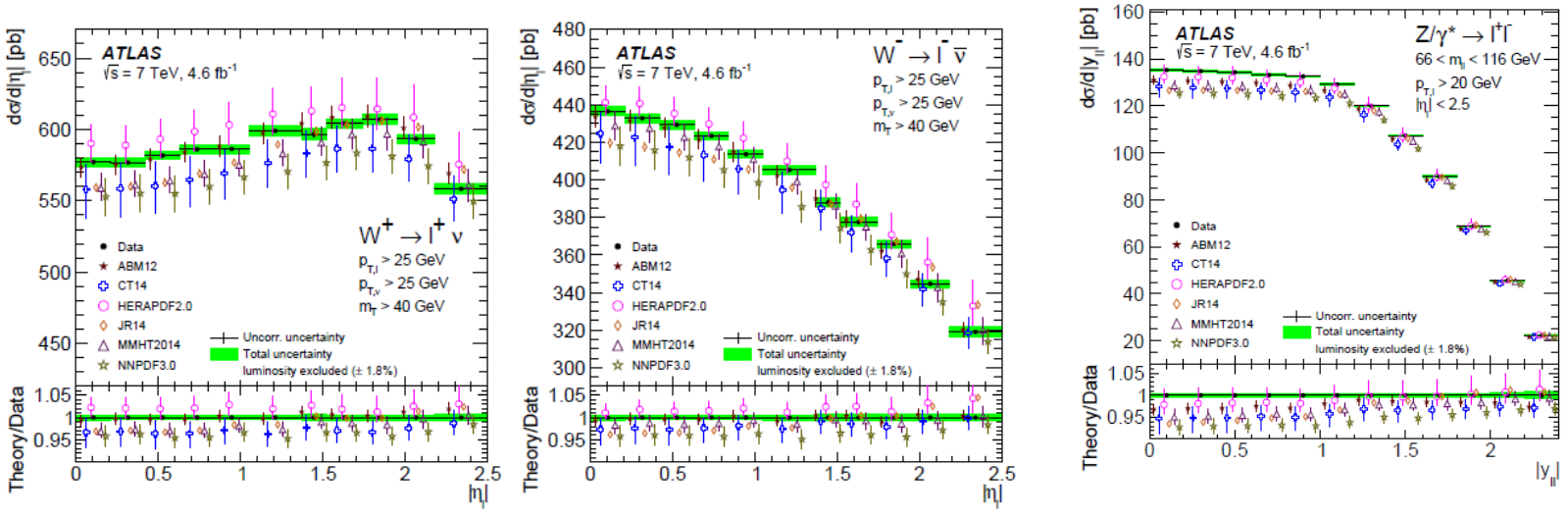

Difficulties in fitting both W and Z distributions fixed by increase in strange quark fraction

$$R_S = \frac{s+\bar{s}}{\bar{u}+\bar{d}}$$

in ATLAS study (PRL 109 (2012) 012001).

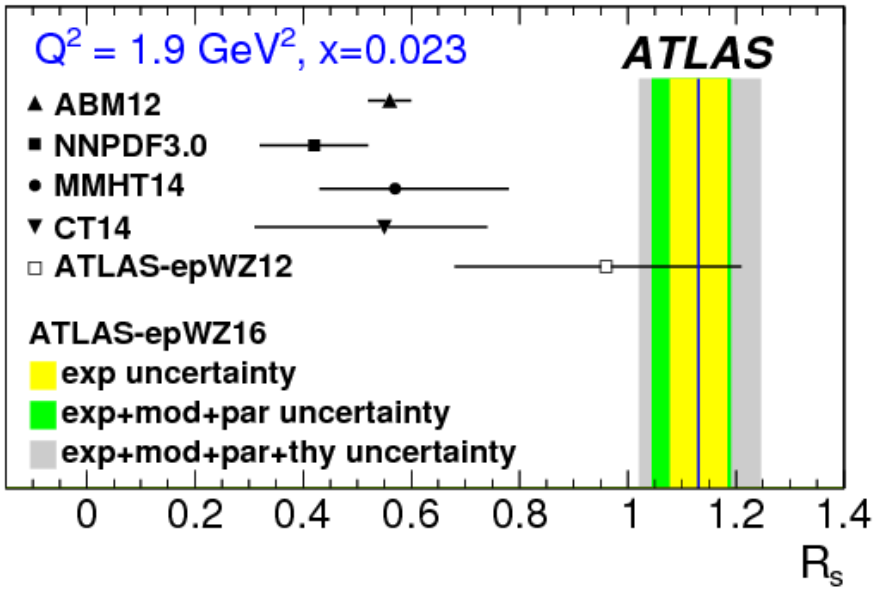

New MSHT2020 PDFs compared to MMHT2014 at NNLO.

Look at $R_s = \frac{s+\bar{s}}{\bar{u}+\bar{d}}$.

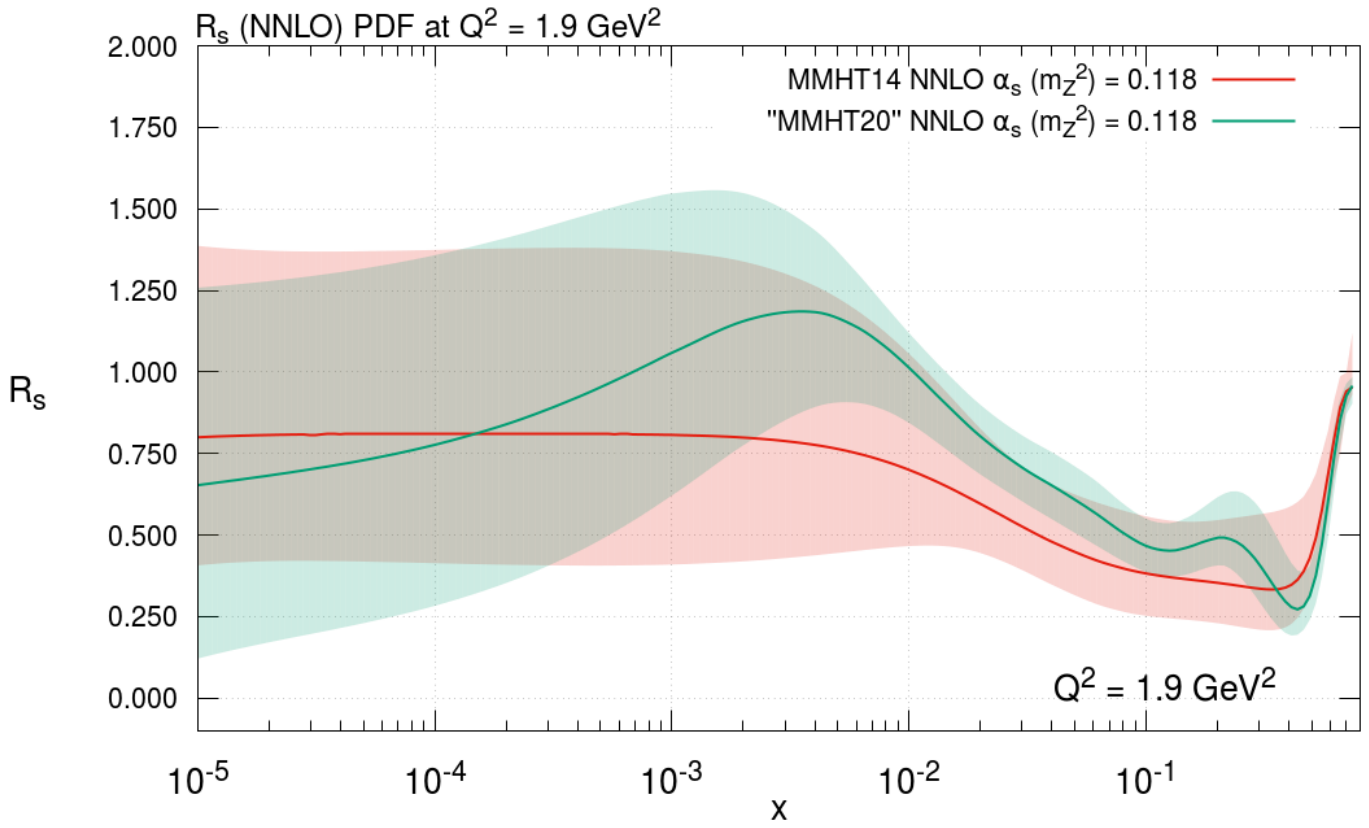

Currently an increase in the strange quark below $x = 0.1$ due to W, Z data (mainly ATLAS 7, 8 TeV).

Still significant uncertainty, and some tension, at higher x. Important constraint from the EIC possible.

High-x Strange Quark.

There is also the possibility of looking at the less well know strange quark via charm quark jets.

Requires dealing with fragmentation (but so do some current methods at some level).

Similar type of data from neutrino scattering on iron targets from CCFR/NuTeV already used.

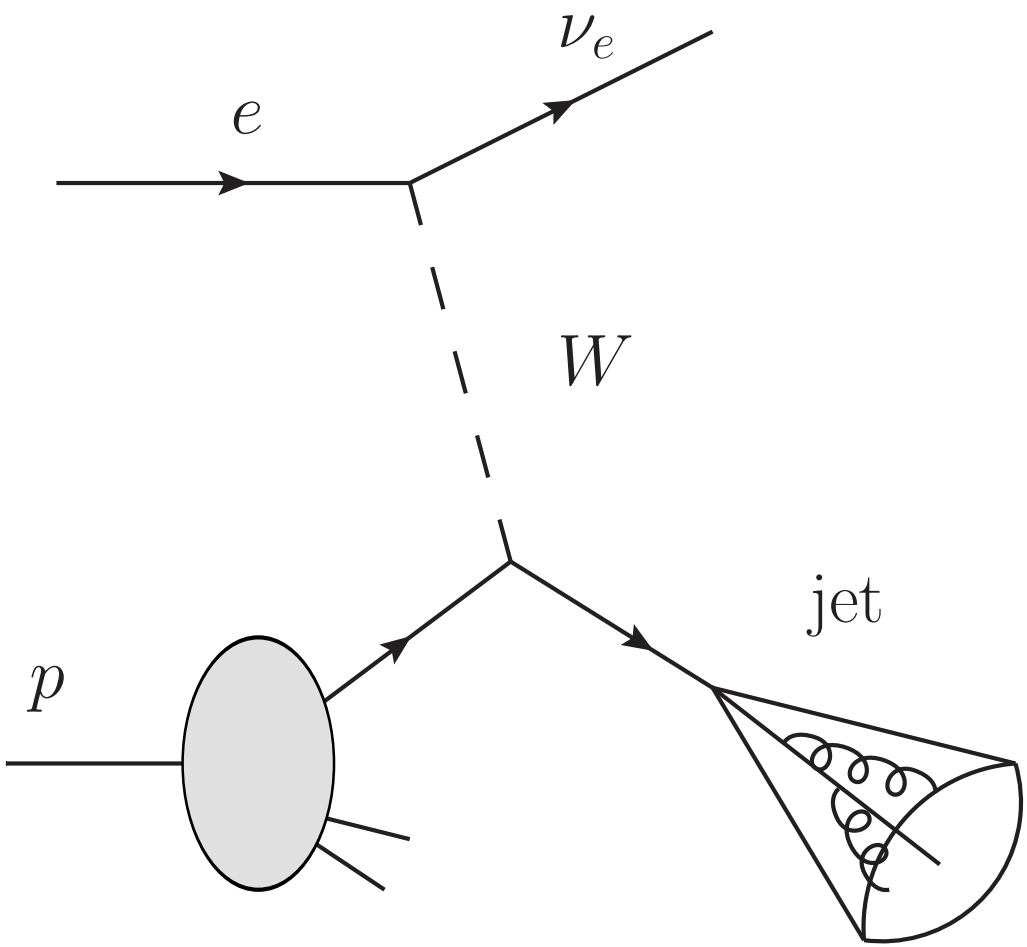

Plot from https://arxiv.org/abs/2006.12520 Arratia et al..

From a CT study one can see the likely x and Q^2 range likely to be covered.

Higher x than the main constraints from the LHC, and from the most precise dimuon measurements.

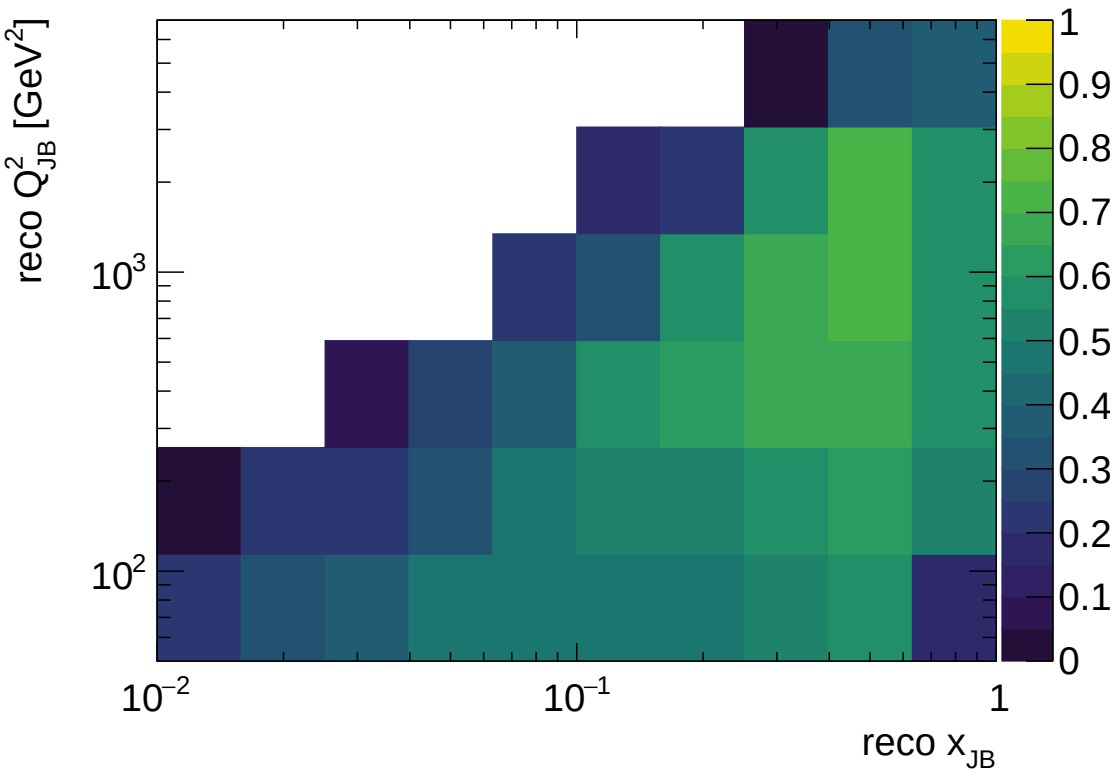

Plot from https://arxiv.org/abs/2006.12520.

Similar, slightly higher energy constraints possible from dimuon production in neutrino DIS at Faser at the LHC (EPJC 80 (2020) 1, 61.)

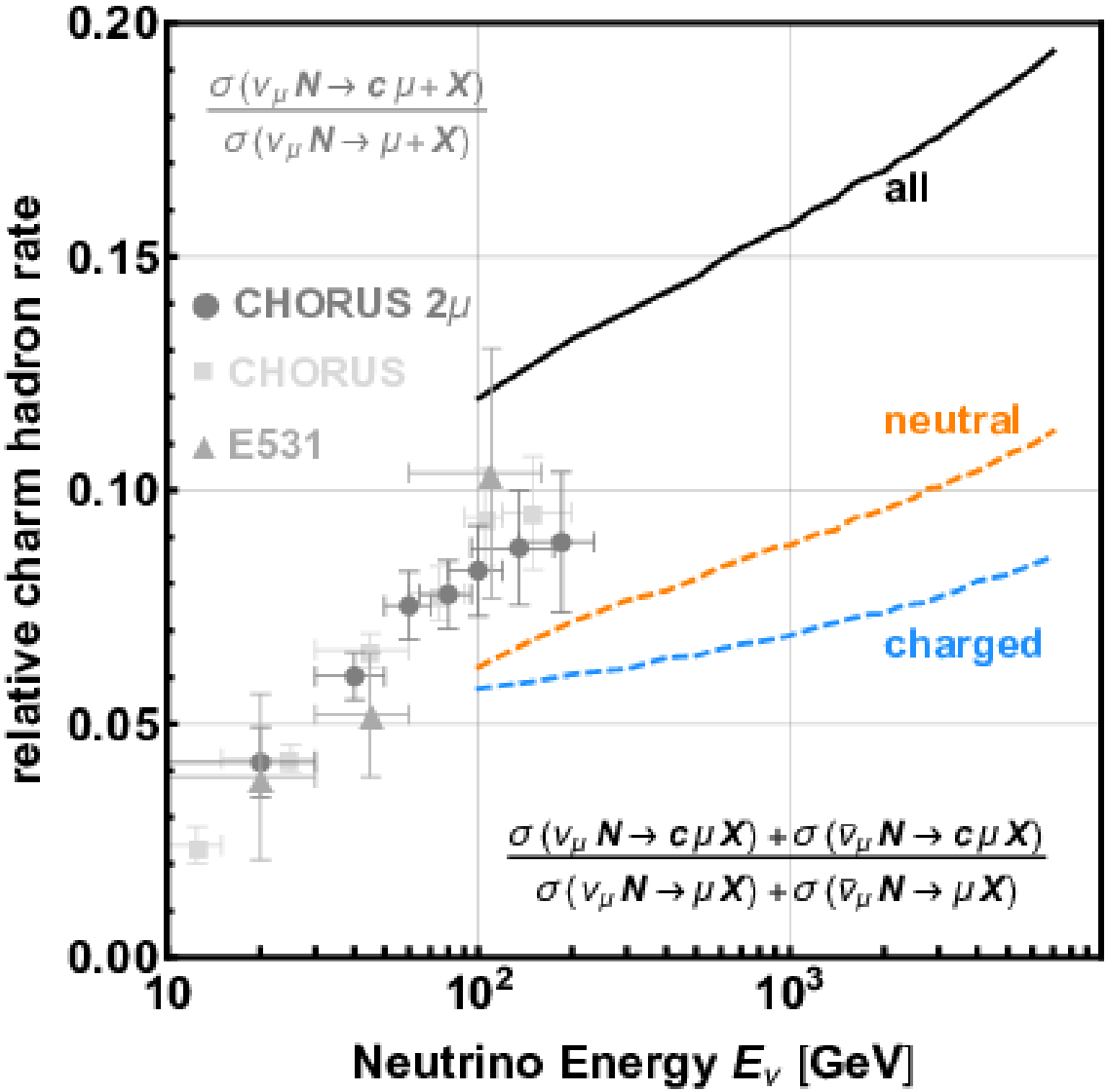

QED corrections and Isospin Violation

Not strictly heavy flavour related, but QED corrections automatically an issue in nuclear PDFs due to isospin violation.

$$\frac{\partial q_i(x,\mu^2)}{\partial \log \mu^2} = \frac{\alpha_S}{2\pi}\int_x^1 \frac{dy}{y}\Big\{P_{qq}(y)\; q_i(\frac{x}{y},\mu^2) + P_{qg}(y)\; g(\frac{x}{y},\mu^2)\Big\}$$
$$+ \frac{\alpha}{2\pi}\int_x^1 \frac{dy}{y}\Big\{\tilde{P}_{qq}(y)\; e_i^2 q_i(\frac{x}{y},\mu^2) + P_{q\gamma}(y)\; e_i^2 \gamma(\frac{x}{y},\mu^2)\Big\}$$

Evolution different for $u(x,Q^2)$ in proton compared to $d(x,Q^2)$ in neutron (and *vice versa*) due to electric charge coupling.

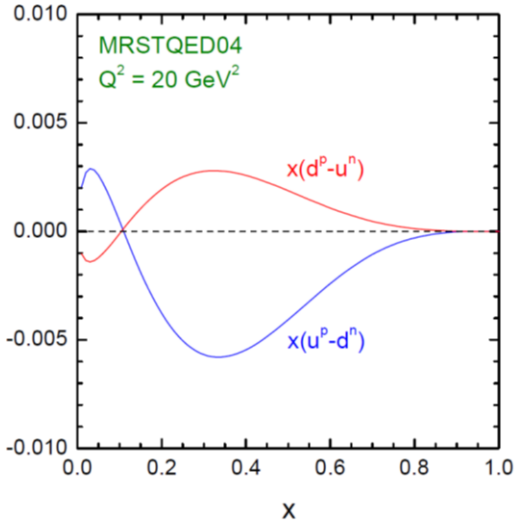

Conclusions

There has been a contribtion to our understanding of heavy falvour physics from numerous DIS experiments over the years.

Wide kinematic range at HERA sensitive to flavour schemes, and to quark masses.

Lower energy experiments can probe the possibility of intrinsic charm, and all experimemts tend to be sensitive to higher twist/nonperturbative effects since m_c is low.

Charged current heavy flavour DIS also gives vital insights into nucleon flavour.

Precision EIC structure function data can potentially make a real impact on pretty much all aspects of this heavy quark physics.

Can also make an impact on the gluon, since this predominantly drives heavy quark production.

A dedicated study on charm jets, mainly producded in the quite far-forward direction, can even improve our knowledge of the strange quark at high x.

Back-up